

HYDRAULIC EFFECT OF SIZE, SPACING AND PATTERN
OF SPACING OF ROUGHNESS ELEMENTS
IN AN OPEN CHANNEL

By

TIMOTHY SOLADOYE KOWOBARI

Bachelor of Science

California State Polytechnic College

San Luis Obispo, California

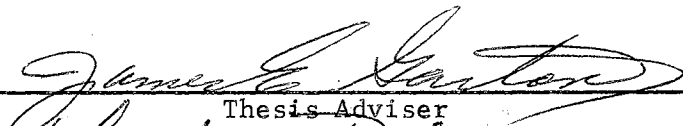
1968

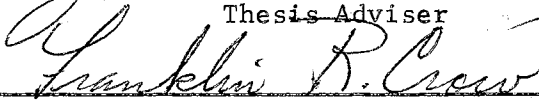
Submitted to the Faculty of the Graduate College
of the Oklahoma State University
in partial fulfillment of the requirements
for the Degree of
MASTER OF SCIENCE
May, 1970


OKLAHOMA
STATE UNIVERSITY
LIBRARY
OCT 12 1970

HYDRAULIC EFFECT OF SIZE, SPACING AND PATTERN
OF SPACING OF ROUGHNESS ELEMENTS
IN AN OPEN CHANNEL

Thesis Approved:



Thesis Adviser




Dean of the Graduate College

762416

ACKNOWLEDGMENTS

The research reported in this thesis was financed in part by the United States Department of the Interior as authorized under the Water Resources Research Act of 1964, Public Law 88-379. This research was conducted as a project of the Oklahoma Water Resources Research Institute, Dr. Marvin T. Edmison, Director. The financial support of the Institute is appreciated.

The author is grateful to the Department of Agricultural Engineering, headed by Professor E. W. Schroeder, for providing assisantships which made this research possible..

A special hearty thanks is extended to the author's adviser, Dr. James E. Garton, for his competent guidance, helpful suggestions and genuine enthusiasm during every phase of this research project.

An expression of gratitude is extended to Professor Charles E. Rice for his comments, suggestions, and assistance during the experimental design and the collection of data stages. Valuable informal discussions and suggestions offered towards the completion of the study by Dr. Richard N. DeVries, Professor of the Civil Engineering Department were appreciated.

The author appreciates the help and services of Mr. John Lewis and many other undergraduate students for the construction of the experimental channel and data collection. Mr. Clyde Skoch, Mr. Norvil Cole and Mr. Jess Hoisington gave valuable technical advice and aid. Mr. Jack Fryrear is acknowledged for his excellent preparation of

illustrative material.

The useful comments and encouragement by Mr. Vincent Uhl, Mr. Glen Carlson and many other fellow graduate students were appreciated.

Finally, I would like to thank Mrs. Karen Metz for her conscientious typing of the thesis.

TABLE OF CONTENTS

Chapter	Page
I. INTRODUCTION	1
Limitations of the Study	3
Objective	3
II. REVIEW OF LITERATURE	5
Gradually-Varied Flow	5
Method of Computation	9
Steady Flow in Open Channel	12
Manning's Equation	13
III. EXPERIMENTAL EQUIPMENT	20
The Channel	20
The Water Supply System	22
The Pumping System	22
The Flow Measurement	24
Depth Measurement Equipment	24
Gage Zero Equipment	27
Artificial Roughness Elements	27
The Common Gage Well	28
IV. METHOD AND PROCEDURE	40
Preliminary Investigation	40
Slope Determination	41
Gage Zeros	41
Testing Procedure	44
V. PRESENTATION AND ANALYSIS OF DATA	46
Bernoulli Energy Equation	47
Dimensional Analysis	49
Pertinent Quantities	50
Channel Roughness without Roughness Elements	53
Channel Roughness with Roughness Elements	53
Prediction of Roughness Coefficient for Gradually- Varied Flow	55
Equation of General Multivariable Response Surface	55
Order of Experimental Analysis	60

Chapter	Page
Identification Technique for Peg Size, Arrangement and Spacing	62
General Discussion on Prediction Equations	66
VI. SUMMARY AND CONCLUSIONS	69
Summary	69
Conclusions	70
Suggestions for Future Study	71
A SELECTED BIBLIOGRAPHY	72
APPENDICES	
APPENDIX A: EXPERIMENTAL DATA FOR THE 3/32-INCH DIAMETER ROUGHNESS ELEMENTS	76
APPENDIX B: EXPERIMENTAL DATA FOR THE 9/32-INCH DIAMETER ROUGHNESS ELEMENTS	80
APPENDIX C: NOMENCLATURE	84

LIST OF TABLES

Table	Page
I. Roughness Coefficients of Channel Lining Material at Varying Slope and Discharge	54
II. Manning's Coefficient, Discharge, and Related Pi-terms for Experiment on Diagonal Grid Spacing of Roughness Elements	56
III. Manning's Coefficient, Discharge, and Related Pi-terms for Experiments on Square Grid Spacing of Roughness Elements	58
IV. Multivariate Exponential Relationship for $n/R^{1/6}$	61
V. Experimental Coefficients, Correlation Coefficient (R) and Standard Deviation (S) of Multivariable Linear Equations for Computing Dimensionless Resistance Coefficients	63
VI. Experimental Coefficients, Correlation Coefficient (R) and Standard Deviation (S) of Multivariable Quadratic Equations for Computing Dimensionless Resistance Coefficients	64
VII. Experimental Coefficients, Correlation Coefficient (R) and Standard Deviation (S) of Multivariable Cubic Equations for Computing Dimensionless Resistance Coefficient	65
VIII. Summary of Correlation Coefficient (R) and Standard Deviation (S) of Multivariable Equations for Predicting Dimensionless Resistance Coefficient	67

LIST OF FIGURES

Figure	Page
1. Derivation of Gradually-Varied Flow Equation	7
2. A Channel Reach for Derivation of Step Method Formula	10
3a. Overall View of Test Channel with 2" x 2" Square Pattern of 3/32-inch Roughness Elements	21
3b. Schematic View of the Experimental Channel	23
4. Sparling Meter Used for Inflow Measurements	25
5. Still Well Device Used for Flow Depth Measurement	26
6. Section View of Test Channel at 4" x 4" Diagonal Spacing of Roughness Elements	29
7. Section View of Test Channel at 2" x 2" Square Spacing of Roughness Elements	30
8. Section View of Test Channel at 2" x 2" Diagonal Spacing of Roughness Elements	31
9. Section View of Test Channel at 1" x 1" Square Spacing of Roughness Elements	32
10. Section View of Test Channel at 1" x 1" Diagonal Spacing of Roughness Elements	33
11. Section View of Test Channel at $\frac{1}{2}$ " x $\frac{1}{2}$ " Square Spacing of Roughness Elements	34
12. General View of Test Channel Showing Low Flow at 2" x 2" Square Spacing of 9/32-inch Roughness Elements	35
13. Overhead View of Channel at 2" x 2" Diagonal Spacing of the 9/32-inch Roughness Elements	36
14. Upstream End View of Channel at 1" x 1" Square Spacing of 9/32-inch Roughness Elements	37
15. Overhead Close-up View of the $\frac{1}{2}$ " x $\frac{1}{2}$ " Square Spacing of the 9/32-inch Roughness Elements	38

Figure	Page
16. General View of Experimental Channel with $\frac{1}{2}$ " x $\frac{1}{2}$ " Square Spacing Under a Flow of 11 g.p.m. and 1 per cent Slope . .	39
17. Gage Zero Determination	42
18. Derivation of Bernoulli Energy Equation	48

CHAPTER I

INTRODUCTION

Flow in open channels has been nature's way of conveying water on the surface of the earth through rivers and streams since the beginning of time. The need for an efficient and practical environment for conveying water resulting from diversions, tailwater, surface run-off, floods, and similar sources within channels has excited the hydraulicians' interest to investigate the natural laws governing water movement in open channel. Irrigation engineers are concerned with transporting water for use on the farm. Traditionally, and in localities where topography permits, the transportation is accomplished by open channels such as main canals, laterals, and farm ditches. The hydrologist is primarily concerned with volume of water and its depth with respect to time and place. Open channel study offers a good guide in the solution of problems such as water movement on farmlands, spillway design for small flood control ponds and reservoirs, highway culvert, vegetated waterway, drainage structures for highways and airport runways.

The amount of water that a channel can convey is governed by the cross-sectional area, the slope, and the resistance coefficient which is dependent on both the material of which the channel is constructed and the maintenance. It cannot be overemphasized that smooth materials will transport water with less resistance than rough surface. The

major problem in channel design has been the determination of the degree of retardance for different boundary conditions. In order to be able to predict or aid the solution of many of the run-off erosion problems, the hydraulic characteristics and performance of the conveyance system must be carefully understood. Information on flow of water through upright stems of real or simulated vegetation is meager.

Although water movement in open channel is one of the earliest of engineering feats, yet no formulas for determining discharges have been developed that are without important limitations. However, formulas have been developed to explain some phenomenon taking place in flow of water in the channel. In the discharge formulas in present use, the resistance coefficient is considered to be constant for a particular type of material in a particular state of upkeep without regard to the other variables. Therefore, there is a great need for more experimental data to better describe the process involved.

In open channel flow, the selection of the hydraulic resistance to flow by both the channel and other roughness elements present poses a problem. This is an important phase of hydraulic research associated with natural streams, floodways and similar channels. Previous investigators in related fields have described the grain-type roughness in wide, open channel. However, it has been found inadequate for describing certain other types of roughness in which the relative size of the roughness elements is an important boundary characteristic.

A review of current literature revealed that most research works on artificial roughness in open channel are restricted to either flows with completely submerged roughness elements with increasing density on variable slope or increasing density at constant slope. It is the

purpose of this experiment to present the results of tests conducted indoors on a smooth rectangular channel fitted with different sizes of artificial roughness element with increasing density, variable pattern and slopes with the hope of making a contribution to better understanding of the degree of retardance in a waterway.

Limitations of the Study

The study was limited to steady state gradually-varied flow. The experimental data were obtained using a 44-foot variable slope rectangular flume located indoors. The flume test width was 1.32 feet. The bottom of channel was lined with 5/16-inch thick aluminum sheet metal. The channel slope was varied from approximately one-fourth to one per cent. The maximum flow ever tested on smooth channel condition without roughness elements was 0.90 c.f.s.

Two sizes of 3/32-inch and 9/32-inch diameter aluminum pegs 3 1/2-inches long were used as roughness elements under two patterns known as diagonal-grid and square-grid system. Mixed size testing was not considered in the experiment. The depth of flow in the channel was limited to unsubmerged condition of the roughness elements.

In the analysis of results, surface velocity and wave-motion effects were not considered. Like most other artificial roughness studies, the upright roughness elements were considered mechanically rigid during the experiment.

Objective

The main objective of this study was to determine the relationship of Manning's resistance coefficient to size of roughness elements,

pattern of arrangement, density of spacing, slope, and discharge in a smooth artificial channel using dimensional analysis and gradually-varied flow.

CHAPTER II

REVIEW OF LITERATURE

Gradually-Varied Flow

Gradually-varied flow is considered a steady state condition in open channels in which the water surface is not parallel to the bottom of the channel. Under this hypothesis, the depth varies gradually along the length of the channel. Among the conditions for gradually varied flow are:

(a) The flow must be steady; i.e., the same flow passes through each cross-section per unit time.

(b) The streamlines are approximately parallel such that hydrostatic pressure exists over the channel section.

According to Chow (3), page 217, the theory of gradually varied flow which dates back to the eighteenth century practically rests on the assumption of:

The head loss at a section is the same as for a uniform flow having the velocity and hydraulic radius of the section. According to this assumption, the uniform-flow formula may be used to evaluate the energy slope of gradually varied flow at a given channel section, and the corresponding coefficient of roughness developed primarily for uniform flow is applicable to the varied flow.

Chow remarked that the assumption above is more correct for varied flow where the velocity increases than where the velocity decreases, because in a flow of increasing velocity the head loss is caused almost entirely by friction effects whereas in a flow of

decreasing velocity there might be a large scale eddy loss.

Theoretical Analysis

Gradually-varied flow can be approached from two methods: The law of conservation of energy and the law of momentum. Both methods are based on Newton's Second law of motion. Chow noted that irrespective of the method of approach the basic assumptions governing Newton's law hold. The two approaches produce practically identical results except that energy conservation is a scalar quantity while momentum conservation is a vector quantity.

Equation of Gradually-Varied Flow

From the profile shown in Figure 1, the total head above the datum at the upstream Section 1 is

$$H = Z + D \cos \theta + \alpha \frac{v^2}{2g} \quad (2-1)$$

where H = Total head in feet

Z = Vertical distance of the channel above the datum in feet

D = Depth of flow section in feet

θ = Bottom slope angle

α = The energy coefficient

V = Mean velocity of flow through the section in feet per second

It must be noted that α and θ are assumed constant throughout the channel reach in question.

Differentiation of Equation (2-1) with respect to reach distance x yields:

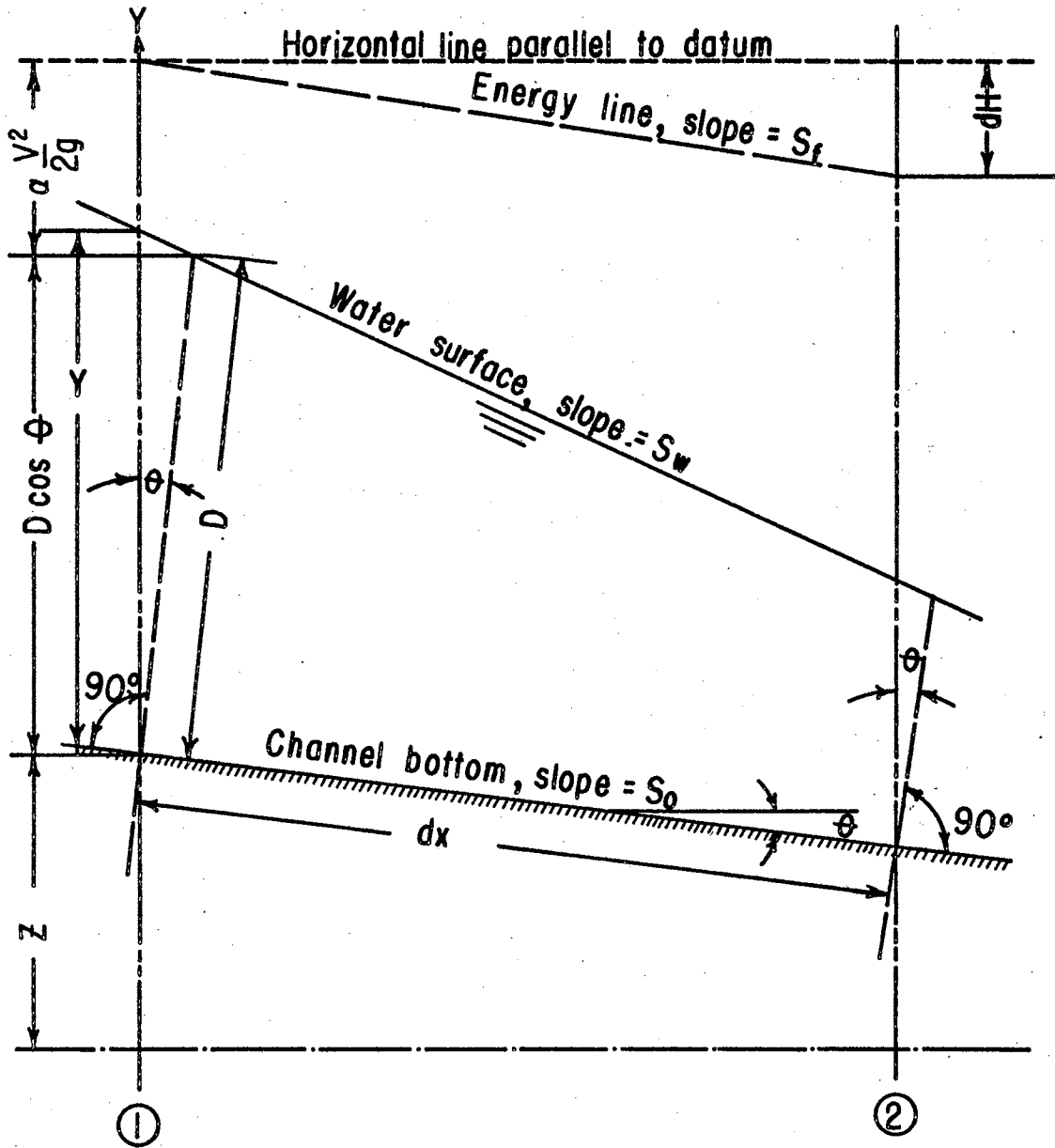


Figure 1. Derivation of the Gradually-Varied Flow Equation
[After Chow]

$$\frac{dH}{dx} = \frac{dZ}{dx} + \cos \theta \frac{d(D)}{dx} + \frac{\alpha d}{dx} \left(\frac{v^2}{2g} \right) \quad (2-2)$$

The channel slope is given by $S_o = \sin \theta = \frac{-dZ}{dx}$. However, θ is assumed a small angle therefore $\sin \theta = \tan \theta = \theta$ radians. Energy slope $S_f = \frac{-dH}{dx}$. Substituting for $\frac{dH}{dx}$ and $\frac{dZ}{dx}$ in Equation (2-2) gives

$$\frac{d(D)}{dx} = \frac{S_o - S_f}{\cos \theta + \alpha \frac{d}{d(D)} \left(\frac{v^2}{2g} \right)} \quad (2-3)$$

Equation (2-3) represents gradually-varied flow. For small angles $\cos \theta \approx 1$, $D \approx y$ and $\frac{d(D)}{dx} \approx \frac{dy}{dx}$.

Hence,

$$\frac{dy}{dx} = \frac{S_o - S_f}{1 + \alpha \frac{d}{dy} \left(\frac{v^2}{2g} \right)} \quad (2-4)$$

The term $\alpha \frac{d}{dy} \left(\frac{v^2}{2g} \right)$ can be recognized as change in velocity head. From the assumption for gradually-varied flow according to Chow(3), page 220, the slope at the channel section of the gradually-varied flow is equal to the energy slope S_f of the uniform flow that has the velocity and hydraulic radius of the section. When the Manning's formula is used, the energy slope is

$$S_f = \frac{n^2 V^2}{2.208 R^{4/3}} \quad (2-5)$$

where n = Manning's roughness coefficient, R = hydraulic radius, V = average velocity of flow.

Method of Computation

The computation of gradually-varied flow profile involves basically the solution of the dynamic equation of gradually-varied flow. The main objective of the computation is to determine the shape of the profile. There are three methods of computation.

1. The Graphical Integration
2. The Direct Integration
3. The Step Method

The latter, for convenience, was used in the analysis of data.

The Direct Step Method

In general a step method is characterized by dividing the channel into short reaches and carrying the computation step by step from one end of the reach to the other. There are several step methods. Some methods are said to be superior to others in certain respects, but no one method has been found to be best in all applications. The direct step method was said to have been suggested by the Polish engineer, Charnomskii, in 1914 and then by Husted in 1924. This is a simple step method applicable to prismatic channels.

With reference to Figure 2 and applying Bernoullis' principle,

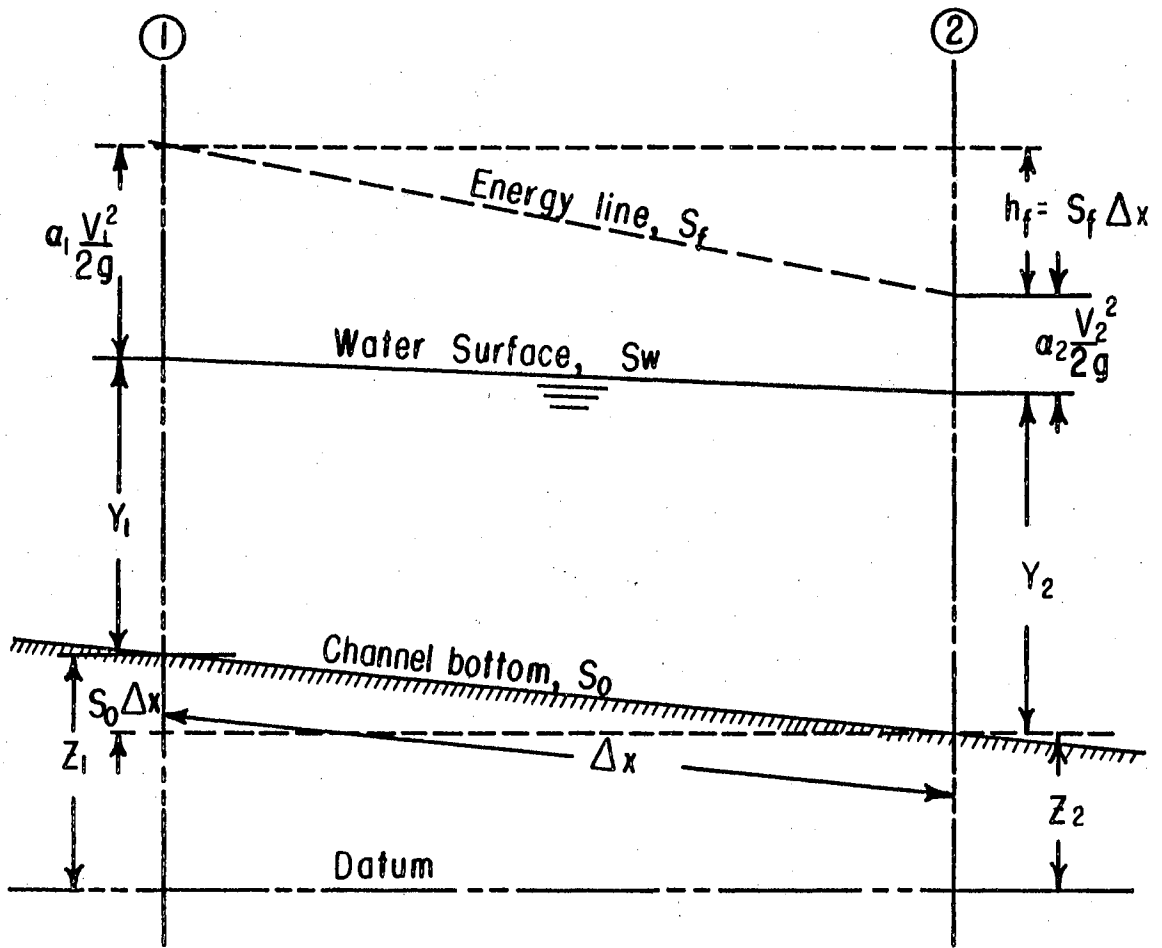


Figure 2. A Channel Reach for the Derivation of Step Method Formula.
[After Chow]

$$S_o \Delta x + y_1 + \alpha_1 \frac{V_1^2}{2g} = y_2 + \alpha_2 \frac{V_2^2}{2g} + S_f \Delta x \quad (2-6)$$

Solving for Δx ,
$$\Delta x = \frac{E_2 - E_1}{S_o - S_f} = \frac{\Delta E}{S_o - S_f} \quad (2-7)$$

where E = Specific Energy at respective stations = $y + \alpha \frac{V^2}{2g}$.

It is assumed $\alpha_1 = \alpha_2 = \alpha = 1$.

Similarly,
$$S_f = \frac{n^2 V^2}{2.208 R^{4/3}}$$

Hendersen (6) also suggested a step method of solution for the energy equation for which he assumed water surface linear so that the average of the friction slopes at the ends of the section under consideration is the average friction slope; i.e., $E_2 - E_1 =$

$$\left[S_o - \left(\frac{S_{f1} + S_{f2}}{2} \right) \right] \Delta x \quad \text{if the two stations are separated by a distance } \Delta x.$$

Assumptions for calculating S_f are:

1. The energy loss varies linearly over the reach Δx under consideration.
2. The energy or Bernoulli equation without velocity distribution coefficient is applicable.

It is to be noted that the error in these assumptions is included in the resistance coefficient. However, regardless of the equation used in calculating S_f , the error due to the assumptions in the momentum equation or the energy equation would finally be absorbed

by the resistance coefficient.

Steady Flow in Open Channel

Hydraulics of steady flow in open channel is an important part of rapidly developing science of hydraulics. Most flows in open channel are turbulent. Turbulence exists when the direction and magnitude of the velocity at any point within a fluid varies irregularly with time. Considerable energy as confirmed by the Soil Conservation Service (24) may be expended in this action. Eddying and "boiling" are visible forms of energy loss. These disturbances in the fluid are produced and maintained largely by roughness and irregularities of the bed and the retardance elements in the system. If the cross-section of the channel does not change along its length, and the channel is straight in alignment and on constant grade, it is said to be uniform channel.

According to Woodward (26) natural water channels are never uniform, but if exceptionally regular, they may be considered to be uniform for some purposes. If the water surface elevation at every section remains the same with respect to time, flow is steady. He emphasized that in using either established Manning's or Kutter's formula for open channel the effect of channel irregularities may be taken into account to a certain extent in estimating the roughness. Lack of parallelism of the water surface and the general grade line of the bottom channel may cause direct application of friction formula to give grossly inaccurate results.

Rouse (20) in open channel resistance studies, suggested that in a basic physical and dimensional consideration of flow characteristics, the following independent variables should be seriously examined:

1. Reynold's Number
2. Relative roughness of the boundary surface
3. Shape of the channel cross-section
4. Degree of non-uniformity of the channel in the profile and in plan.
5. Froude Number
6. Degree of unsteadiness of flow

In fact, he stressed that unsteady open channel flow is broadly regarded as a combination of boundary resistance and wave motion. The wave limit is very complicated and any problem involving both to comparable degree is still essentially too complex for more than rough analysis, Rouse concluded.

Sayre (22) in his analysis pointed out the role of Reynolds number. In fact, if the magnitude of the roughness is large compared to the thickness of the lamina sublayer, the viscous effect would be negligible, and consequently, the Reynolds number would be of less importance. In such a case a boundary hydrodynamical roughness condition is said to exist.

Manning's Equation

Accurate determination of discharge in open channels requires, within reasonable limit, an estimate of the degree of retardance, usually known as coefficient of roughness. Early research in this area though not a systematic study, was prompted by the hydraulics of open channel trying to keep pace with roughness studies in closed conduit which was at an advanced stage of development. There are two major formulas for computing discharge in open channel. The first

was developed by Chezy in 1775. He was acknowledged as the first engineer to observe the effect of channel roughness through his equation

$$V = C \sqrt{RS} \quad (2-8)$$

where R = Hydraulic radius of the channel

S = Slope of the channel

V = Velocity of flow

C = Coefficient of roughness

The second which is widely used in the United States is Manning's formula first introduced in 1891, as a classic foundation stone of modern open channel hydraulics. In an attempt to correlate and systematize existing data from natural and artificial channels, Manning proposed an equation which was later developed into

$$V = \frac{1.486}{n} R^{2/3} S^{1/2} \quad (2-9)$$

where V = Velocity of flow

R = Hydraulic radius

S = Frictional slope

n = Coefficient of resistance

Rouse (21) pointed out that these empirical formulas including Ganguillet and Kutter formula known as:

$$C = \frac{1.486}{n} R^{1/6} \quad (2-10)$$

are not without limitations, though they give fair results when applied over fairly narrow range of conditions on which they were based, but they frequently lead to serious errors with applications outside their range.

The resistance coefficient as observed by (10), (11), and (13); however, is not a constant for a given channel but varies with velocity and depth.

As a result of these inconsistencies several investigators have made studies using artificial roughness elements, each using a different type of roughness for the purpose of determining the retardance of flow for the particular type of roughness chosen. Most of these investigators made partial attempts to understand and establish the phenomena taking place when a degree of roughness is present.

Sayre and Albertson (23) gave a discussion on the results of early experiments by G. H. Keulegan, Nikuradse and Einstein in an effort to establish roughness standard for wide, open channels. Their approaches have been reported to be quite successful in describing the grain-type roughness in wide, open channels. However, the approaches have been found inadequate for describing certain other types of roughness in which the relative spacing in addition to relative size of the roughness elements is an important boundary characteristic.

In the above category is Powell's (10) method in which he used square strips extending across the bed of the test channel as roughness in studying the effect of the longitudinal spacing of the strips.

Robinson and Albertson (18) in an attempt to establish a

reproducible artificial roughness standards that would be applicable to open channels claimed a huge success from their study. In their experiment, the sizes of geometrically similar roughness baffles were varied in spacing while the ratios of longitudinal and transverse spacing to baffle heights were held constant. Placement was such that each baffle was centered on the openings between baffles in the rows immediately upstream and downstream. Tests were conducted with roughness baffles of two sizes. These baffle sizes were 1-inch high by 4-inches wide and $\frac{1}{2}$ -inch by 2-inches long. Traverse spacings were twice the baffle height, and longitudinal spacings were ten times the baffle height, so that for both baffle sizes, identical patterns of roughness were formed. For a particular roughness pattern they demonstrated that the Chezy resistance function depends only on relative roughness (ratio of flow depth to baffle height) assuming rough boundary conditions. As a result of this investigation a resistance formula was established in the form

$$c = 26.65 \log_{10} (1.891 d/a) \quad (2-11)$$

where c = Resistance coefficient

d = Mean depth of flow

a = Height of artificial roughness

In this experimental result it was also claimed that a staggered pattern of individual roughness baffles proved extremely effective in maintaining large sediment concentrations in suspension without appreciable deposit, whereas extensive deposits occurred at comparable concentrations when the roughness consisted of baffles

extending continuously across the width of the flume.

In natural open channels, a situation of composite roughness exists whereby one or more than one type of resistance element is encountered. This situation occurs frequently when a flooding river overflows its banks. It is not unlikely for dead bodies of animals, detritus, rocks, and sewage to create a high degree of retardance. This subject in its entirety could become a complicated problem. This aspect though was not covered in this particular study; it might be implied. Einstein and Bank (4), however, studied the effect of composite roughness in a channel having:

1. Concrete blocks laid parallel to the floor of channel.
2. Concrete blocks combined with $\frac{1}{4}$ -inch diameter by $1\frac{1}{2}$ -inch high pegs with various peg densities and pattern.
3. Blocks with alternative blocks offset $\frac{1}{4}$ -inch.
4. Blocks with alternate blocks offset, and combined with various peg densities and pattern.

They finally established equations for resistance exerted by the bed of the channel in terms of the density of roughness elements and the square of the velocity of flow. For example, the resistance equation for the block and peg experiment was found to be

$$T_{bp} = (0.00505 + 0.00175 N) V^2 \quad (2-12)$$

where T_{bp} = Resistance of blocks and pegs in lbs/ft^2

V = Velocity of flow

N = Density of pegs

Of course the equations developed were assumed to be valid as long as different roughness elements do not exert mutual interference on the flow.

Fang (5), on the hydraulic effect of grasses that have upright stems on the retardance of flow in open channels, sodded eight flat bottomed earth channels described as unit channels with Sudan grass vegetation. Each channel was 3-feet wide and 96-feet long with considerable steep slope of five per cent. The channel material was silt loam soil of 82.0 lbs/ft³ average density. Plant population was estimated and discharges through the channel were measured at different stages of growth. Using dimensional analysis approach as well as Manning's formula, he developed the following relationship

$$\frac{R^{1/6}}{n} = A + \frac{B}{\sigma_b ND} \quad (2-13)$$

where A and B are some numerical constants to be determined by experiment for particular conditions.

N = population of plants in the flow per square foot of the channel bottom.

n = Coefficient of retardance of the channel.

D = Mean diameter of plant stems in the flow.

R = Hydraulic radius of the channel.

σ_b = Standard deviations of the bottom variation computed from the bottom readings of the point gage.

It was stated that the equation is only applicable to

unsubmerged vegetation that has considerably clean, upright stems in the flow of moderate velocity.

Johnson (9), on a study of artificial roughness in open channels, used rectangular wooden block nailed to the bottom of a redwood flume to determine the coefficient of resistance to flow. In this study he plotted the Manning's roughness factor against the ratio between the spacing and the height of the rough elements and found that at a minimum ratio of spacing to depth of element, the roughness factor reached a maximum and beyond this point, the factor decreases.

Ree (12) (13), along with his other experiments performed both at Spartanburg, South Carolina, and Stillwater, Oklahoma, has contributed practical and useful information to the solution of grassed channels. He emphasized how Manning's n for one kind of vegetation varied over a wide range depending on the depth of flow and the slope of the channel. In his experiment he reported results of flow retardance coefficients for several row-planted crops. He related the Manning's n for a growth to the product of velocity and hydraulic radius when the velocities were great enough to displace the vegetation.

Boyer (1), using height of roughness as a means of estimating the roughness coefficient for natural channels, obtained results which were considered to be within acceptable limit of accuracy. It was observed that not only does the roughness height, but the sinuosity as well have a bearing on the magnitude of the coefficient of retardance.

CHAPTER III

EXPERIMENTAL EQUIPMENT

The system consists of the test channel, the pumps, the pipelines, storage sump, settling tank, water meters, common stilling well, point gages and a thermometer. The artificial roughness elements were made of circular aluminum rods. The whole experimental equipment was located indoors at the Oklahoma State University, Agricultural Engineering Research Laboratory.

The Channel

The channel consists of a 44-foot long, 18-by 7½-inch steel WF beam which was supported on its side as shown in Figure 3a to form a variable slope rectangular flume. The bottom was lined with 5/16-inch thick aluminum sheet metal which was built to fit snugly at the bottom. This was facilitated by a cutting at a 45-degree angle on the side edges of the lining. These bottom linings were in 6-foot sections. Tight joints between the sections were secured with epoxy. The channel effective width inside the side panneling was 1.32 feet. The channel slope was adjusted by variable height supports. These were pipe stands with holes at calculated intervals for adjusting the slope within the range desired. Shims were used to get the desired elevation.

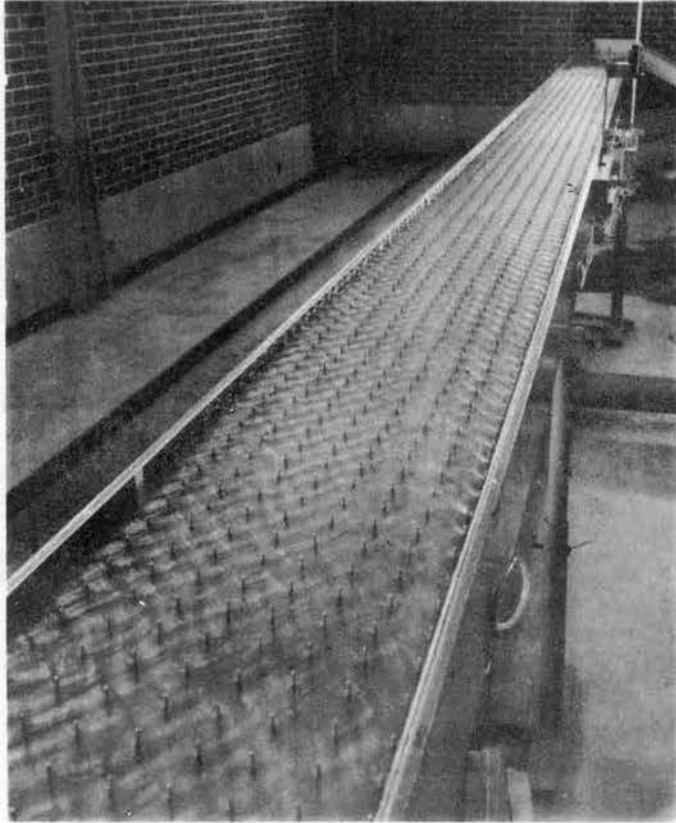


Figure 3a. Overall View of Test Channel
with 2" x 2" Square Pattern
of 3/32-inch Roughness
Elements

The Water Supply System

The source of water was a large 9-foot long by 5-foot wide by 5-foot deep storage sump sunk at the lower end of the channel. A 9-foot long by 18-inch wide by 6-inch deep sheet metal flume was connected between the lower end of the channel and the sump. Circulated water dropped into a tailbox connected between the flume and the channel before it was conveyed to the sump. Two water supply pipeline systems were used. A 2-inch pipeline was used for discharges up to 100 gallons per minute while a 6-inch pipe was used for flows above 100 gallons per minute. The two pipes were respectively connected to discharge into a common stilling tank of 2-feet by 2-feet by 3-feet located at the upstream end of the channel before water was emptied into the channel through a spout as shown in Figure 3b. Turbulence of the entering flow was reduced by forcing water to flow through a contraction thereby creating a backwater upstream before flowing over a 2-inch by 2-inch wooden block and finally through 8 and 16 mesh aluminum screens. The screen device also served as catchment device for rust coming out of supply pipelines.

Pumping System

The pumping system consists of a $\frac{1}{2}$ -horse power motor driven Bell and Cossett 1531 Type B pump connected to 2-inch pipe and a $7\frac{1}{2}$ -horsepower motor driven Berkeley pump connected to the 6-inch line. Both pumps were centrifugal pumps.

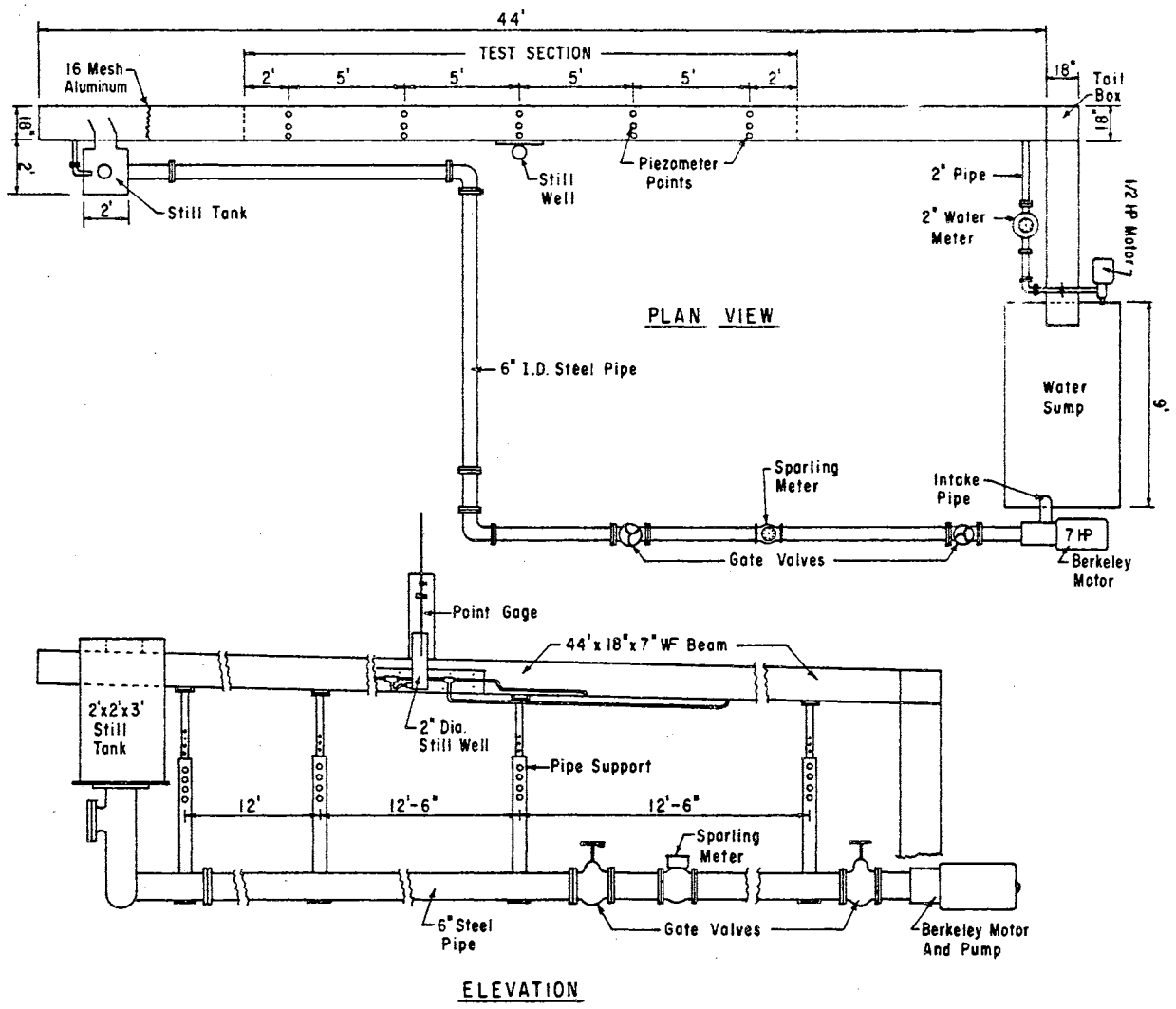


Figure 3b. Schematic View of the Experimental Channel

Flow Measurement

Small inflow into the experimental channel was measured with a 2-inch nutating totalizing disc water meter incorporated in the 2-inch pipeline. Large discharge over 100 gallons per minute was measured with the Sparling meter shown in Figure 4. The Sparling meter was calibrated with a sharp edge orifice and U-tube manometer at the outdoor hydraulic laboratory near Stillwater, Oklahoma. The meter was installed in the 6-inch line. With a stop watch, calibration of the water meter on the 2-inch line was made by collecting the outflow in a bucket for a certain time period. Laboratory scale was used to obtain the weight of the water and bucket. A correlation between actual and observed discharges was established at low flows.

Depth Measuring Equipment

A common stilling well and point gage system as shown in Figure 5 was located at a station about 0 + 21-feet down the channel from the upstream end. By having water surface elevations at desired stations referenced to a common stilling well, errors in point gage, bench mark readings, and oscillatory water elevation could be reduced to a bare minimum. Five depth measuring stations for water surface elevations were located at distances 0 + 11, 0 + 16, 0 + 21, 0 + 26, and 0 + 31-feet along the channel from the upstream end. At each station, three brass plugs with holes of about 0.07 inch bore were used as piezometer taps to measure the flow depth. The brass plugs were set level with the inside bottom of the channel and they protruded from the lower side of the steel beam. Each of the three plugs placed in line at each station commanded an equal field area across

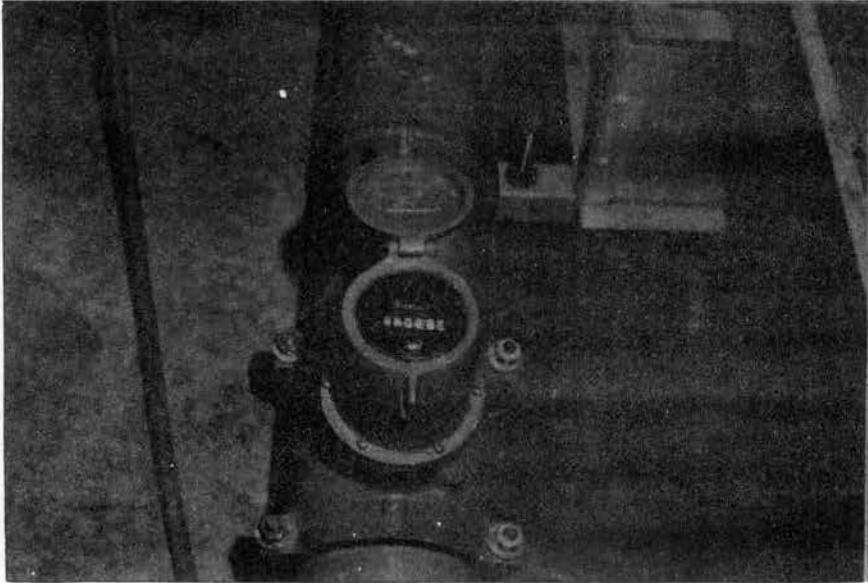


Figure 4. Sparling Meter Used for Inflow Measurements

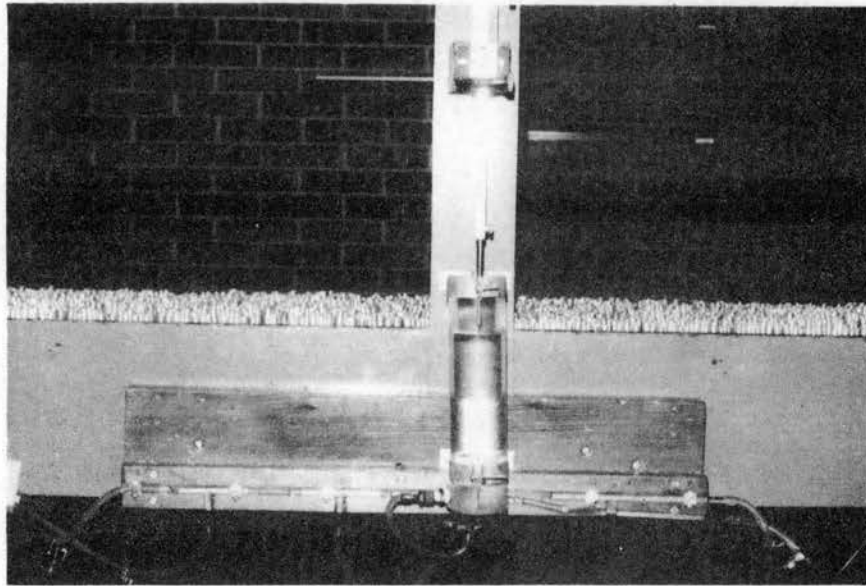


Figure 5. Still Well Device Used for Flow Depth Measurements

the channel. Initially the bottom ends of these piezometers had been counterbored to cut down surface tension and capillary effect. Rubber and brass tubings connected the piezometers in an assembly from each station as a common unit before eventually making connection to the stilling well.

Gage Zero Equipment

An engineer's level was used to find the elevation of the central brass plugs at each station for bottom profile readings along the channel. A point gage with a blunt end was utilized as a rod gage. Shims were used in adjusting the channel slope.

Artificial Roughness Elements

There were two sets of sizes of artificial roughness elements for this experiment. The elements consisted of round and smooth aluminum rods of sizes 3/32-inch and 9/32-inch diameter cut into small pegs 3 1/2 inches long. Holes of the same diameter as the pegs under test were drilled 1/4-inch deep into the channel bottom lining. The pegs were driven into holes drilled sequentially at definite longitudinal and transverse spacings to form patterns known as Diagonal grid and Square grid systems. In this experiment two different patterns and six types of spacings excluding bare channel lining condition were studied. Schematics of the six types of spacings are shown in Figures 6 through 16.

The Common Gage Well

The common gage well unit consists of a 9-inch long 2-inch inside diameter plexi-glass tube sealed at one end to form a well. Tygon plastic tubings from the peizometer stations were attached in an assembly with T-joint glass tubing and a common connection was made to the well. The well was centrally located from the test ends of the channel. A common point gage was supported at this central location for water surface elevation measurement in the gage well as shown in Figure 5.

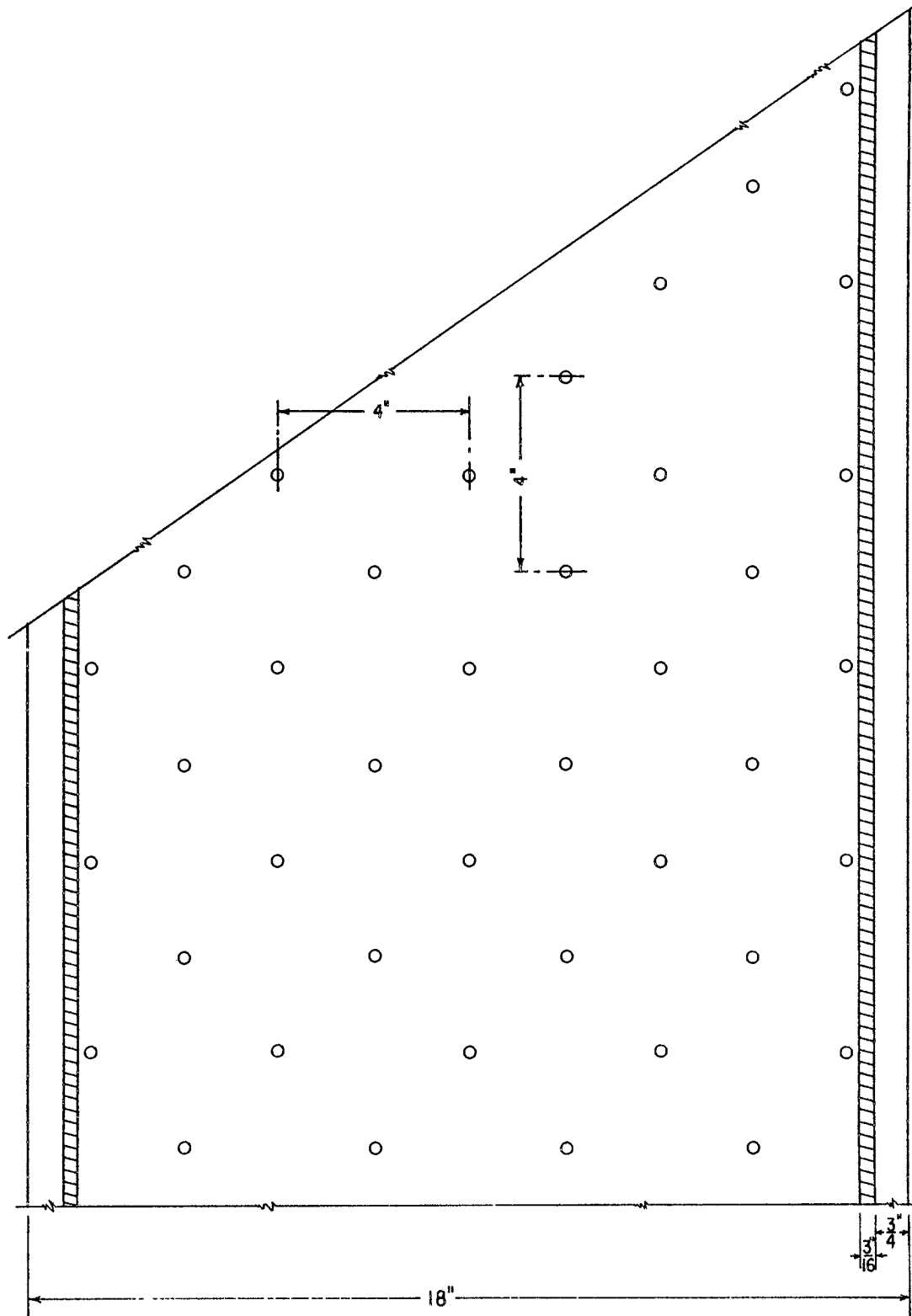


Figure 6. Section View of Test Channel at 4" x 4" Diagonal Spacing of Roughness Elements

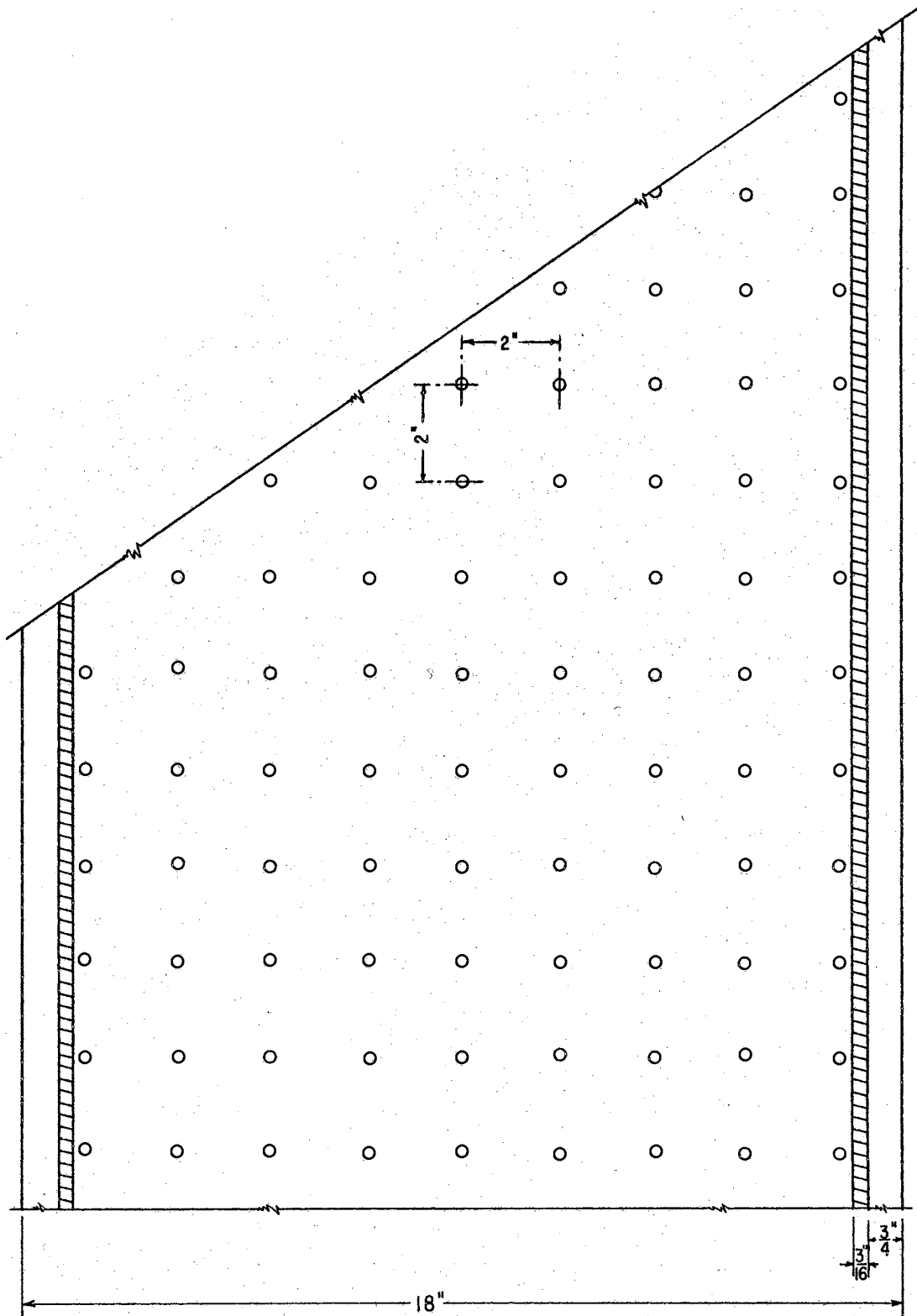


Figure 7. Section View of Test Channel at 2" x 2" Square Spacing of Roughness Elements

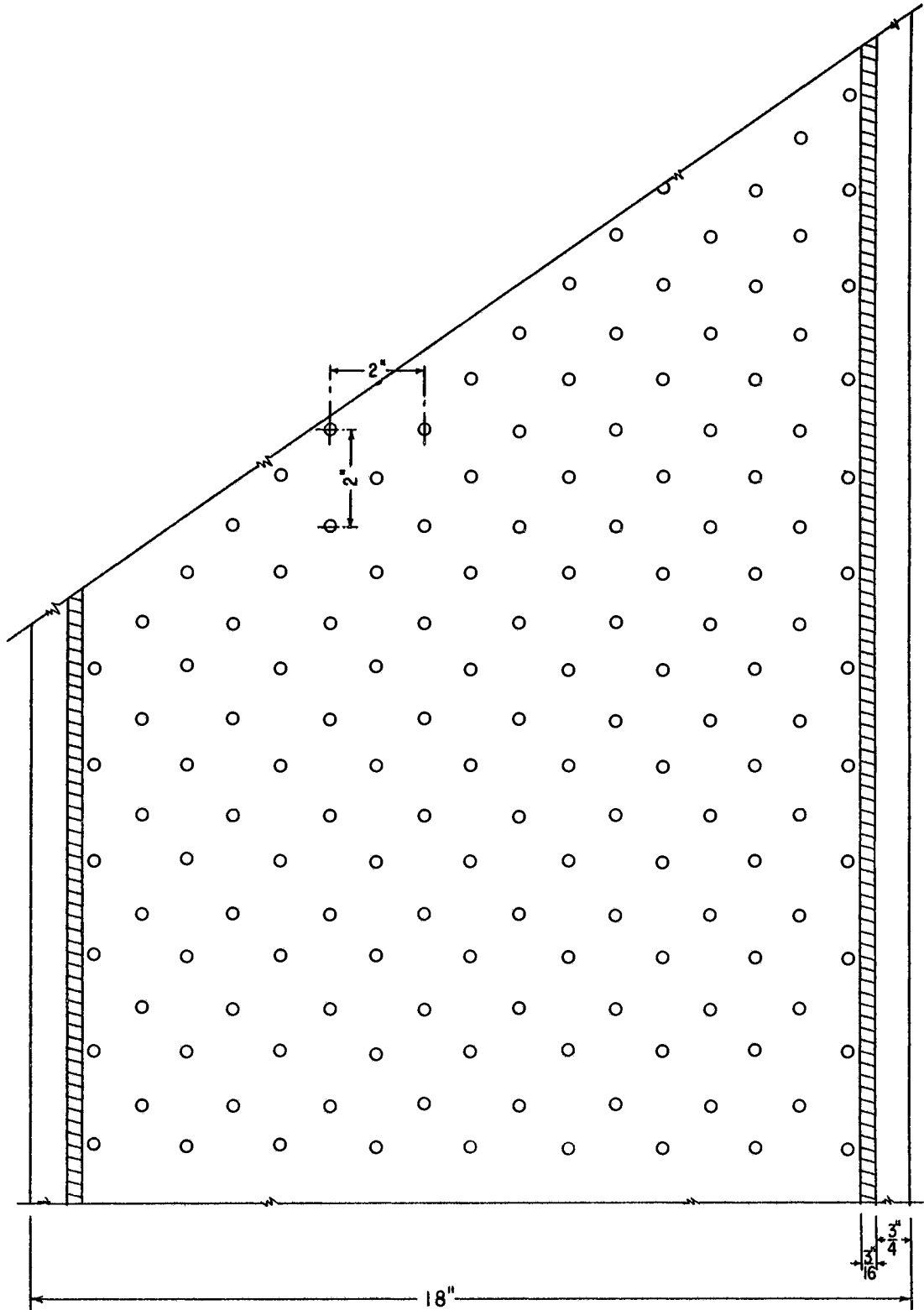


Figure 8. Section View of Test Channel at 2" x 2" Diagonal Spacing of Roughness Elements

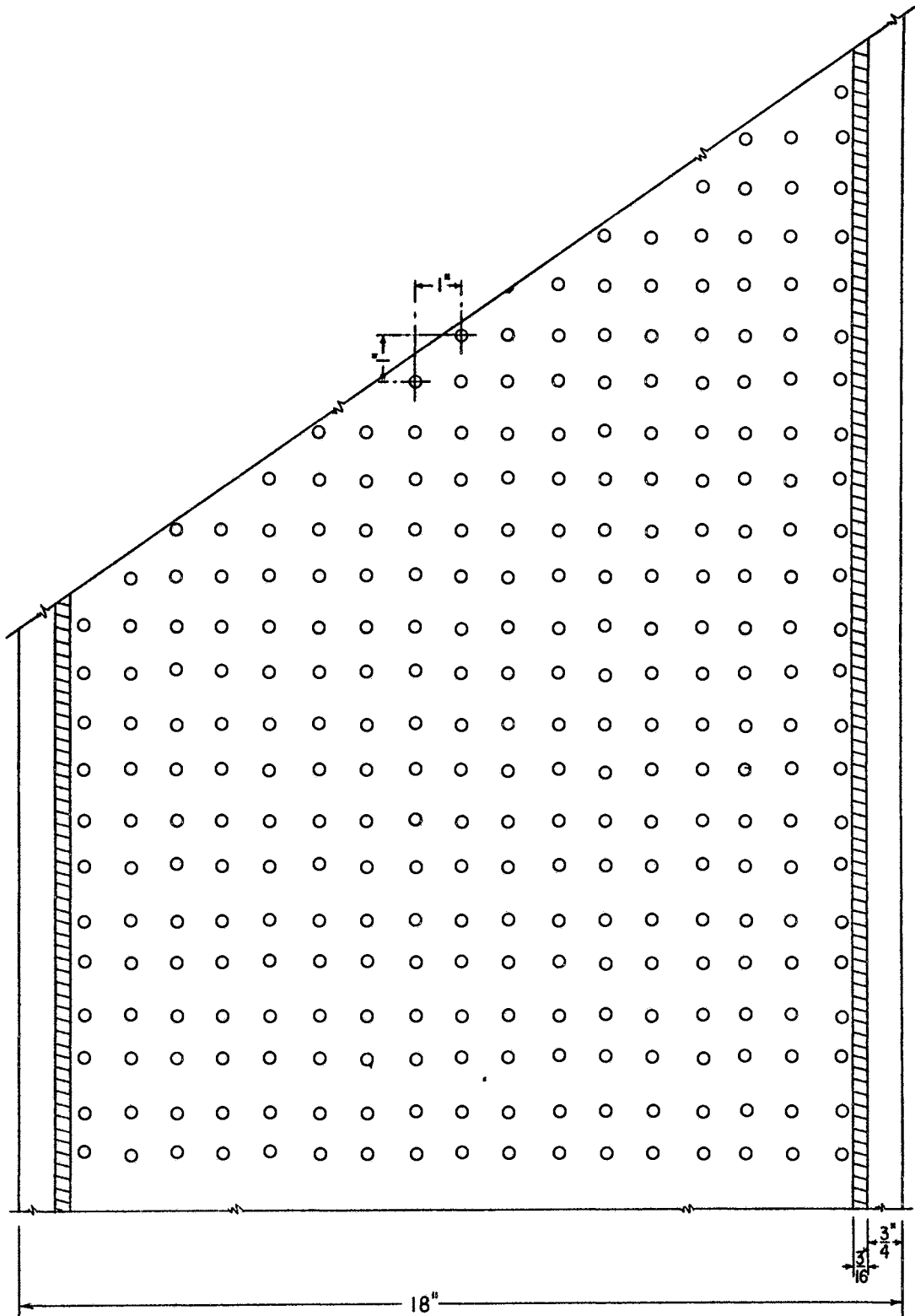


Figure 9. Section View of Test Channel at 1" x 1" Square Spacing of Roughness Elements

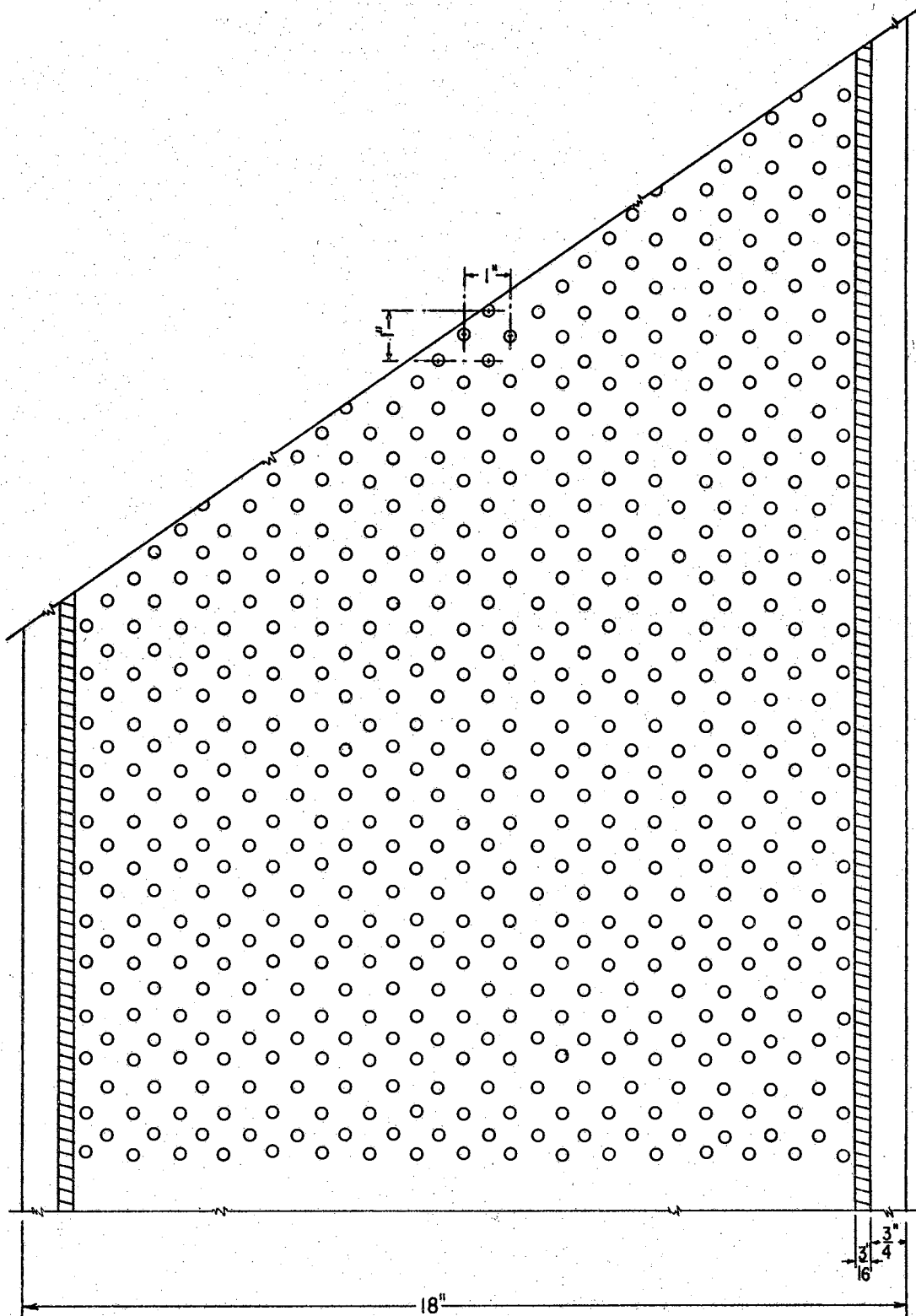


Figure 10. Section View of Test Channel at 1" x 1" Diagonal Spacing of Roughness Elements

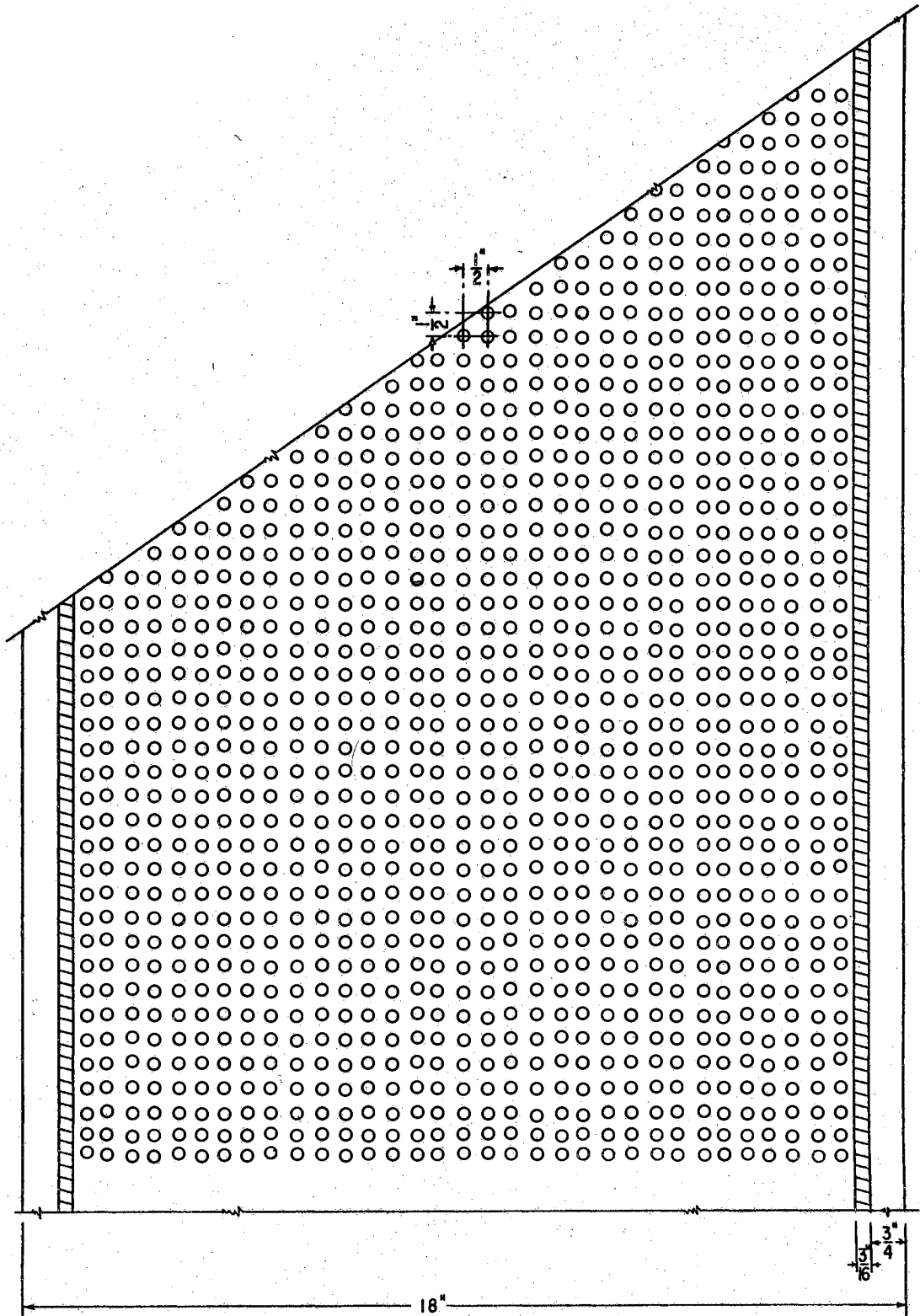


Figure 11. Section View of Test Channel at $\frac{1}{2}$ " \times $\frac{1}{2}$ " Square Spacing of Roughness Elements

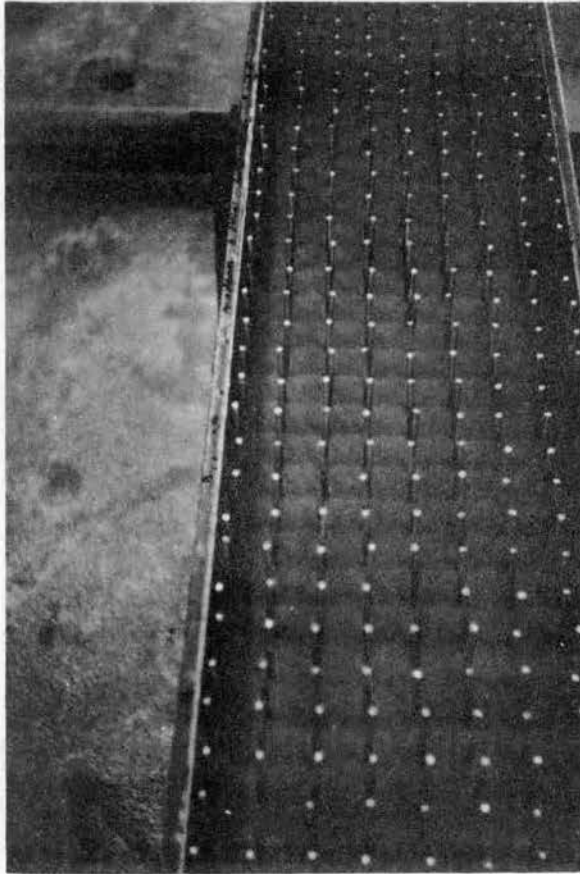


Figure 12. General View of Test
Channel Showing Low
Flow at 2" x 2" Square
Spacing of 9/32-inch
Roughness Elements

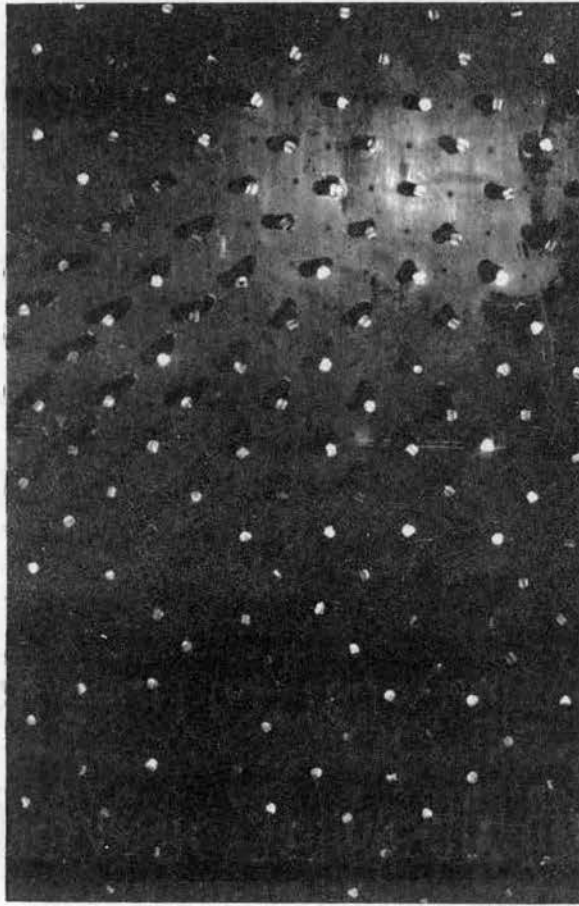


Figure 13. Overhead View of Channel
at 2" x 2" Diagonal
Spacing of the 9/32-inch
Roughness Element

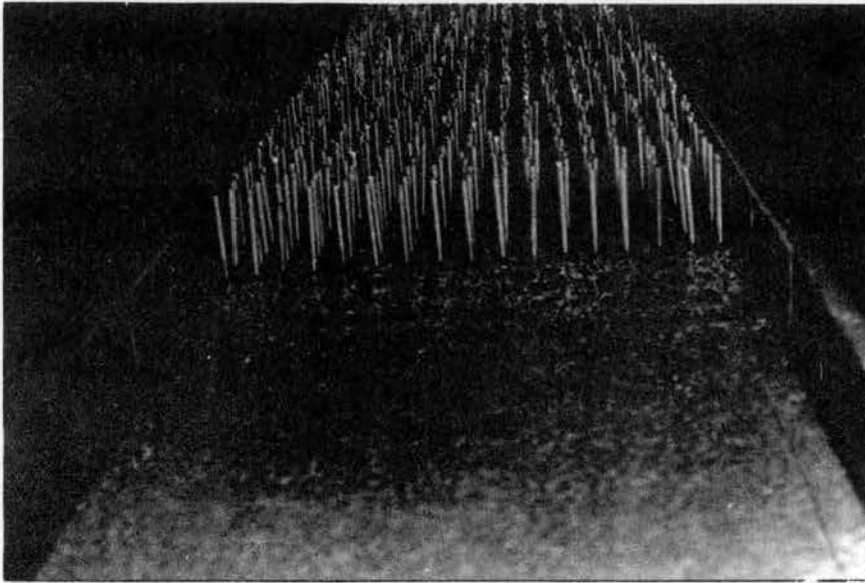


Figure 14. Upstream End View of Channel at 1" x 1"
Square Spacing of 9/32-inch Roughness
Element

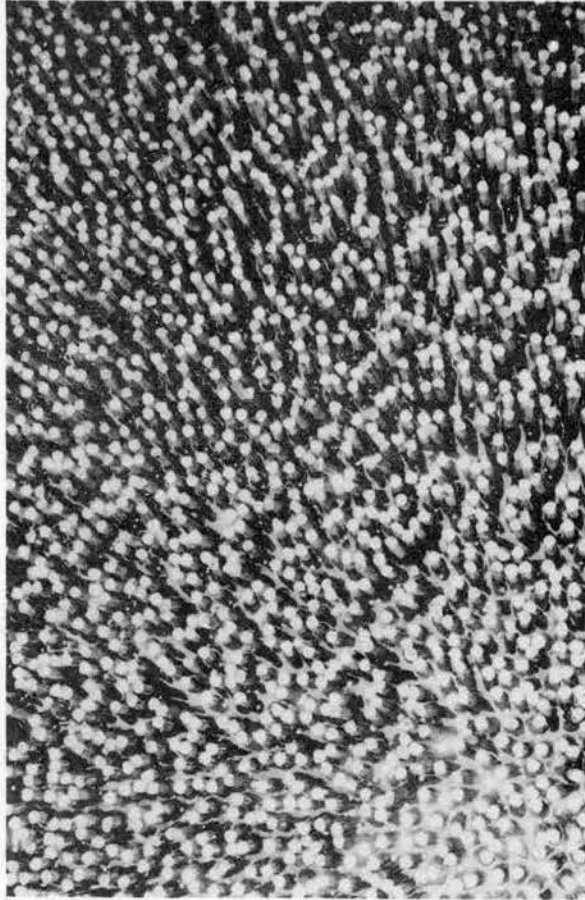


Figure 15. Overhead Close-up View of
the $\frac{1}{4}$ " x $\frac{1}{4}$ " Spacing of
the $\frac{9}{32}$ -inch Roughness
Elements

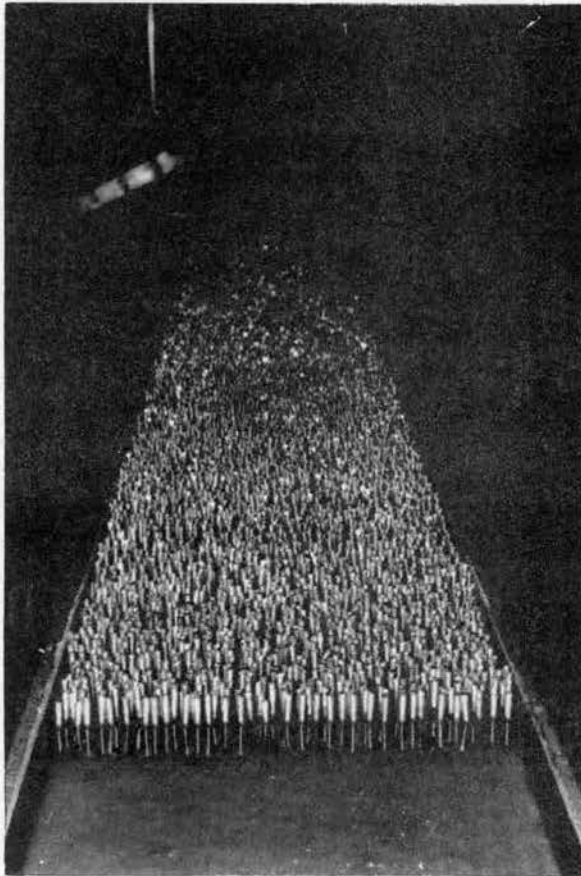


Figure 16. General View of Experimental Channel at Element Spacing of $\frac{1}{2}$ " x $\frac{1}{2}$ " Under a Flow of 11 g.p.m. and 1 per cent Slope

CHAPTER IV

METHOD AND PROCEDURE

Preliminary Investigation

A preliminary investigation of the use of a 5/8-inch thick plywood as a testing base for the channel was conducted. Interior-grade plywood was cut into sizes to fit tightly into the WF-beam in 4-foot sections. The surface was waxed and coated with three layers of varnish to provide a smooth and water-proof bottom. The plywood sections were carefully secured in place inside the channel with contact cement and the joints between the sections were sealed off to make water-tight joints. The sides of the WF-steel beam channel was coated with gray latex paint. Piezometers were sunk inside the plywood and steel beam at regular station intervals. The bottom profile of the new bottom lining was taken while there was water running and also when water has been run through. Repeated examination of the bottom profile plot of elevation versus distance downstream showed irregularities in the profile of about four-thousandth of a foot as a result of variable moisture absorption and swelling of the interior-grade plywood. It was decided to discontinue using the plywood bottom for the tests because larger errors might result from swelling and shrinkage of the plywood after a long time.

Alternatively, and as a matter of convenience, it was decided to use ALCOA 313-thousandth inch thickness aluminum sheet metal for the

bottom lining and 140-thousandth inch thick aluminum sheet for the side paneling of the channel.

Slope Determination

The slope of the experimental channel was established by using shims in conjunction with the variable channel support adjustment. In this operation screw jacks were used to prop the channel. The elevation of the central brass piezometers at each station was referenced to a permanent bench mark located in the experimental laboratory. These relative elevations were determined using an engineer's level and a blunt-end point gage as a rod gage. The approximate desired slope was rechecked by taking the bottom profile of the channel. Adequate care was taken to see that each time the slope was changed, the central point gage at the common stilling well was plumbed with a carpenter's level. Corresponding adjustment of the height of the tailbox at the discharge outlet into the sump was made with each change of slope.

Gage Zeros

Two point gages A and B as shown in Figure 17 were used in establishing the gage zeros. A gage zero was the elevation of the point gage tip when the zero mark on the point gage shaft coincided with the zero mark on the vernier scale. In the experiment point gage A was used for measuring water surface elevation while point gage B was used for taking channel bottom profile. A separate gage zero was established for each point gage. The engineer's level was used for establishing the gage zeros by adhering to the following procedures:

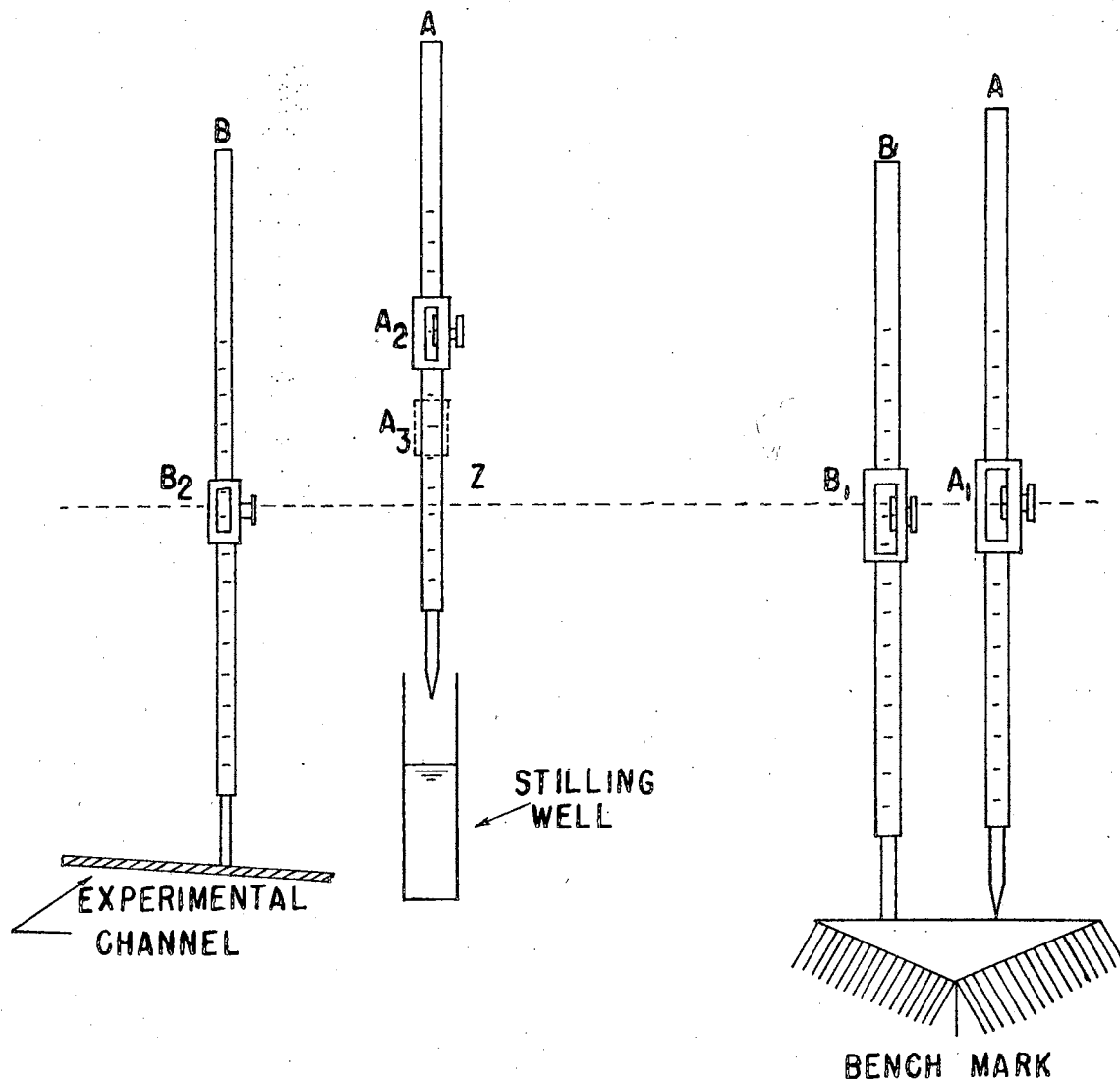


Figure 17. Gage Zero Determination

1. Level readings of point gages A and B were taken on a non-yielding support known as the bench mark. Earlier, arbitrary elevation of the bench mark was assumed as 10.000 feet.

2. Point gage A was placed in its bracket at the common gage well and a convenient foresight Z was established. At the same time corresponding vernier readings A_2 were registered.

3. Rod zeros (the elevations of the point gage tip that would occur if the horizontal instrument crosshair were reading 0.000 feet on the point gage shafts) were calculated for each point gage.

$$\begin{aligned} \text{Rod Zero for gage A} &= (\text{Elevation of Bench Mark}) - (\text{Level Reading at} \\ &\hspace{15em} \text{Bench Mark}) \\ &= 10.000 - A_1 \end{aligned}$$

$$\begin{aligned} \text{Rod Zero for gage B} &= (\text{Elevation of Bench Mark}) - (\text{Level Reading at} \\ &\hspace{15em} \text{Bench Mark}) \\ &= 10.000 - B_1 \end{aligned}$$

4. Gage Zeros were calculated as:

$$\begin{aligned} \text{Gage Zero for gage A} &= \text{Rod Zero} - (\text{Vernier Reading} - \text{Foresight}) \\ &= (10.00 - A_1) - (A_2 - Z) \\ &= (10.00 + Z) - (A_1 + A_2) \end{aligned}$$

$$\text{Gage Zero for gage B} = \text{Rod zero for B} = 10.00 - B_1$$

5. Level Readings B_3 of the central piezometers at each station were taken with point gage B and vernier reading A_3 was read when the point gage A just touched the water surface in the stilling well.

6. Calculation of depth of flow:

$$\begin{aligned} \text{Flow depth} &= (\text{Gage Zero A} + A_3) - (\text{Gage Zero B} + B_2) \\ &= (Z + B_1 + A_3) - (A_1 + A_2 + B_2) \end{aligned}$$

Testing Procedure

Essentially the procedure consisted of passing five measured flows down the test channel and making all observations needed to compute the hydraulic elements of the channel. The five successive discharges at every slope condition were made in order of increasing magnitude.

At a particular slope, water was pumped into the upstream end of the channel. Five to ten minutes was allowed for the flow to attain equilibrium condition. The initial stream was controlled in such a way to give a minimum depth of flow of above $\frac{1}{4}$ -inch to reduce surface tension effect each time the flow rate was changed. After equilibrium condition, discharge was measured for two minutes on the 2-inch meter and for five minutes on the spurling meter. The discharge reading was repeated at the end of each experimental run and the average value was calculated. The water surface elevation at each station was measured at the common stilling well with a common point gage. The point gage reading of the water surface at each station was taken in sequence starting from the downstream station to the upstream end. Care was taken to see that all water lines but one under test was closed with a Mohr pinch clamp during each point gage vernier reading. An interval of three to five minutes was allowed for water in the stilling well to reach a steady state after changing station. All point gage measurements were read to 0.001 foot. During the test, the regime and flow conditions were carefully observed and the temperature of water during the test was recorded in degrees Fahrenheit. From measurements taken, the cross-sectional area, the wetted perimeter, and the hydraulic radius for each run was

determined. Values of roughness coefficient was calculated for each 5-foot test reach between stations. The average value of the roughness coefficient for the channel was determined.

CHAPTER V

PRESENTATION AND ANALYSIS OF DATA

Uniform steady state gradually-varied flow tests were conducted to determine the hydraulic effect of the size, spacing and pattern of the roughness element on resistance to flow of water in the test channel. The University IBM 360 Computer and Olivetti Underwood Programma 101 Computer were used for calculations necessary in the analysis. The Manning's equation as in Equation (5-1) was used to calculate the hydraulic roughness coefficient.

$$n_{(r \rightarrow r+1)} = \left[\frac{2.208}{V_m^2} (R^{4/3})_m \left(\frac{\Delta E}{\Delta L} + S_o \right) \right]^{\frac{1}{2}} \quad (5-1)$$

where $(R^{4/3})_m$ = Arithmetic average of hydraulic radius between two adjacent piezometric stations raised to 4/3 power

V_m = Average velocity of flow between two adjacent piezometric stations

ΔE = Difference in the total energy head due to depth and velocity of flow between adjacent reaches.

ΔL = Channel reach between two stations

S_o = Average channel slope between the reach

$n_{(r \rightarrow r+1)}$ = Hydraulic roughness coefficient between adjacent reaches

Bernoulli Energy Equation

The energy equation results from the application of the principle of conservation of energy to fluid flow. The energy possessed by a flowing fluid consists of internal energy and energies due to pressure, velocity and position. In the direction of flow, the energy principle is summarized by a general equation as follows:

$$\begin{array}{ccccccccc} \text{Energy at} & & \text{Energy} & & \text{Energy} & & \text{Energy} & & \text{Energy at} \\ \text{Station 1} & + & \text{Added} & - & \text{Lost} & - & \text{Extracted} & = & \text{Section 2} \end{array}$$

This equation, for steady flow of incompressible fluids in which the change in internal energy is negligible, simplified to Equation (5-2) according to Figure 18.

$$y_1 + \frac{v_1^2}{2g} + z_1 = y_2 + \frac{v_2^2}{2g} + h_L \quad (5-2)$$

But $Z = S_o \Delta x$ and similarly $h_L = S_f \Delta L$.

$$\text{Therefore, } y_1 + \frac{v_1^2}{2g} + S_o \Delta x = y_2 + \frac{v_2^2}{2g} + S_f \Delta L.$$

Recognizing $y + \frac{v^2}{2g}$ as the sum of pressure and velocity energies, the change in energy ΔE between stations 1 and 2 is

$$y_1 + \frac{v_1^2}{2g} - y_2 - \frac{v_2^2}{2g} = (S_f - S_o) \Delta L$$

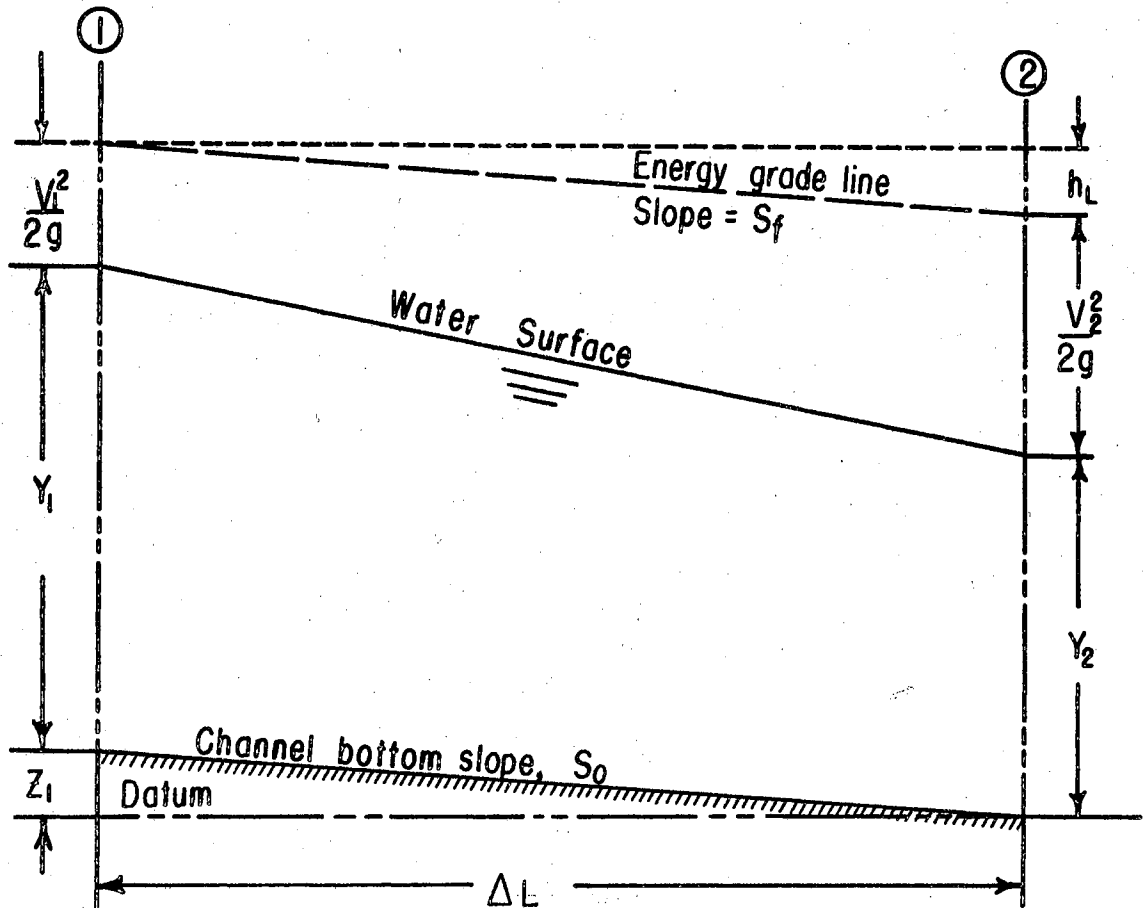


Figure 18. Derivation of Bernoulli Energy Equation

Therefore, $\frac{\Delta E}{\Delta L} = S_f - S_o$

Hence, $S_f = \frac{\Delta E}{\Delta L} + S_o$

Substituting for S_f in the Manning's Formula

$$V_m = \frac{1.486}{n} R^{2/3} S_f^{1/2}$$

$$V_m = \frac{1.486}{n} R^{2/3} \left(\frac{\Delta E}{\Delta L} + S_o \right)^{1/2}$$

By rearrangement

$$n = \left[\frac{2.208}{V_m^2} \left(R^{4/3} \right)_m \left(\frac{\Delta E}{\Delta L} + S_o \right) \right]^{1/2}$$

Dimensional Analysis

Dimensional analysis is a very powerful tool in experimental design. It has two major advantages.

1. It saves time by allowing the experimenter to obtain useful data with a minimum of experimental and computational effort.
2. The possibility of describing all the contributing factors of a physical system by a single equation.

In this analysis, dimensions of Force - Length - Time approach called F-L-T was employed. Variables known as pertinent quantities thought to be contributors to the hydraulic phenomenon of the problem were selected with designations listed.

Pertinent Quantities

No.	Symbol	Quantity	Dimensions
1	n	Roughness coefficient	L
2	V	Mean velocity	LT^{-1}
3	D	Depth of flow	L
4	S	Slope of channel	--
5	b	Channel width	L
6	L	Channel test length	L
7	g	Acceleration due to gravity	LT^{-2}
8	λ	Shape factor defining type of stem	--
9	δ	Factor denoting roughness pattern	--
10	N	Average number of stems/row	--
11	B	Density of stem per square foot	L^{-2}
12	d	Stem diameter	L
13	l	Stem length	L
14	K	Stiffness modulus of stem	FL^2
15	ρ_s	Stem density per unit length of stem	$FL^{-2}T^2$
16	ρ	Fluid density	$FL^{-4}T^2$
17	μ	Fluid viscosity	$FL^{-2}T$

The general functional relationship between the quantities can be written:

$$f(n, V, D, S, b, L, g, \lambda, \delta, N, B, d, l, K, \rho_s, \rho, \mu) = 0$$

(5-3)

From Buckingham Pi-theorem (7) there are seventeen pertinent quantities. Therefore, fourteen dimensionless groups could be formed. Choosing V , D and ρ as repeating variables, the possible dimensionless groups are expressed as the function in Equation (5-4)

$$f\left(\frac{n}{D^{1/6}}, \frac{d}{b}, \frac{L}{b}, \frac{D}{b}, \frac{\lambda}{b}, s, \delta, \lambda, \frac{\rho d^2}{\rho_s}, \frac{K}{\mu_d^{7/2} g^{1/2}}, dBD, \frac{Nd}{b}, \frac{V^2}{gD}, \frac{\rho VD}{\mu}\right) = 0 \quad (5-4)$$

Simplification and Limitation of Functions for Study

A complete solution of this function was impossible because of the large number of variables involved and the amount of time required.

In this analysis some of the primary quantities or combinations were held constant, and the remaining ones varied to study their effects on the secondary quantities. The criteria for elimination were by their expected importance and influence on the experiment.

From physical limitations of the design some assumptions were made:

1. The roughness elements will not be completely submerged at any time; thus, λ can be eliminated from consideration.
2. The elements are assumed to be stiff and unyielding when put in place; therefore, the value of K and ρ_s would remain constant.
3. The term δ has only three values for smooth channel condition, Square grid and Diagonal grid conditions.

4. The term λ defining shape has only one condition which is circular; therefore, the effect would be constant throughout the experiment.

5. For a steady state condition the term $\frac{L}{b}$ remains constant.

6. The effect of roughness remains almost constant at high Reynolds number for turbulent flow condition.

The terms containing λ , K , ρ_s , δ , and λ may be considered to be of secondary importance.

Thus, Equation (5-4) becomes

$$f\left(\frac{n}{D^{1/6}}, dDB, \frac{D}{b}, \frac{Nd}{b}, s, \frac{V^2}{gD}\right) = 0$$

or

$$f\left(\frac{n}{R^{1/6}}, dDB, \frac{D}{b}, \frac{Nd}{b}, s, \frac{V^2}{gR}\right) = 0 \quad (5-5)$$

After replacing the terms $\frac{n}{D^{1/6}}$, $\frac{V^2}{gD}$ and $\frac{\rho VD}{\mu}$ by $\frac{n}{R^{1/6}}$, $\frac{V^2}{gR}$, and

$\frac{VR}{\sqrt{\nu}}$ respectively where

$$\sqrt{\nu} = - \left[\frac{\log_{10} T - 2.333}{0.4609 \times 10^5} \right]$$

T = Temperature degrees Fahrenheit, and R = Hydraulic radius of the channel.

The function in Equation (5-5) can be arranged in pi-terms for convenience as follows:

$$\pi_1 = \frac{n}{R^{1/6}} \quad - \quad \text{Dimensionless Roughness Coefficient}$$

$$\pi_2 = dDB$$

$$\pi_3 = \frac{D}{b}$$

$$\pi_4 = \frac{Nd}{b}$$

$$\pi_5 = S$$

$$\pi_6 = \frac{V^2}{gR} \quad - \quad \text{Froude Number}$$

Channel Roughness without Roughness Elements

A series of gradually-varied flow experiments was designed to measure the hydraulic resistance of the bottom lining. Five different discharges were tested at each average channel slope of 0.0023, 0.0044, 0.0050 and 0.0091. The Manning's Equation (5-1) was used to calculate Manning's roughness coefficient for every reach of the channel. An average channel value of the roughness coefficient was determined for each discharge. The values of the roughness coefficient 'n' are listed in Table I. In general, the values of Manning's 'n' decreased with an increase in discharge. The observed mean channel roughness coefficient was 0.0086. The deviation from the mean of the observed values was generally in the order of 3.5 per cent though scanty cases gave 11.5 per cent deviation.

Channel Roughness with Roughness Elements

Gradually-varied flow studies were conducted on six different types of spacings and patterns of roughness elements shown in

TABLE I
ROUGHNESS COEFFICIENTS OF CHANNEL LINING
MATERIAL AT VARYING SLOPE AND DISCHARGE

Slope	Discharge (CFS)	Roughness Coefficient
0.0023	0.0638	0.0094
	0.1208	0.0088
	0.1597	0.0083
	0.2200	0.0086
	0.3496	0.0084
0.0044	0.1013	0.0094
	0.1419	0.0091
	0.1998	0.0088
	0.2305	0.0088
	0.4164	0.0086
0.0050	0.3385	0.0086
	0.4565	0.0083
	0.6570	0.0082
	0.7639	0.0083
	0.8841	0.0081
0.0091	0.0821	0.0094
	0.1351	0.0087
	0.2231	0.0086
	0.3763	0.0076
	0.4031	0.0078

Figures 6 through 11. The afore-mentioned six dimensionless groups as well as Reynolds number were calculated for every discharge as reported in Tables II and III.

Prediction of Roughness Coefficient for Gradually-Varied Flow

As a result of several parameters varying at the same time during each test, three computer programs were designed to fit a multivariable response surface equation with no interaction for the six variables in Equation (5-5). These equations were in linear, quadratic and cubic forms. In all programs, provision was made for a least square linear regression analysis of observed and calculated values of dimensional roughness coefficient π_1 , in terms of $\pi_2, \pi_3, \pi_4, \pi_5$ and π_6 for every discharge condition. Coefficient of correlation and standard deviation between observed and calculated values of π_1 were also determined.

Equations of General Multivariable Response Surface

The polynomial equations are of the form:

$$\text{Linear: } Y = C_1 + C_2X_1 + C_3X_2 + C_4X_3 + C_5X_4 + C_6X_5 \quad (5-6)$$

$$\begin{aligned} \text{Quadratic: } Y = & C_1 + C_2X_1 + C_3X_1^2 + C_4X_2 + C_5X_2^2 + C_6X_3 + C_7X_3^2 + C_8X_4 + \\ & C_9X_4^2 + C_{10}X_5 + C_{11}X_5^2 \end{aligned} \quad (5-7)$$

TABLE II

MANNING'S COEFFICIENT, DISCHARGE, AND RELATED PI-TERMS FOR EXPERIMENT
ON DIAGONAL GRID SPACING OF ROUGHNESS ELEMENTS

Spacing Ident.	Discharge (CFS)	dDB	$\frac{D}{b}$	$\frac{Nd}{b}$	s	$\frac{v^2}{gR}$	$\frac{n}{R^{1/6}}$	'n'
D-4	0.1230	0.0193	0.0750	0.0296	0.0022	0.3208	0.0230	0.0152
	0.1857	0.0271	0.1055	0.0296	0.0022	0.2770	0.0258	0.0178
	0.2325	0.0317	0.1230	0.0296	0.0022	0.2820	0.0265	0.0187
	0.2962	0.0374	0.1453	0.0296	0.0022	0.2890	0.0278	0.0201
	0.3229	0.0392	0.1524	0.0296	0.0022	0.3019	0.0281	0.0205
D-4	0.0291	0.006	0.0235	0.0296	0.0051	0.559	0.0247	0.0136
	0.1297	0.0159	0.0618	0.0296	0.0051	0.624	0.0236	0.0151
	0.2320	0.0259	0.1005	0.0296	0.0051	0.4956	0.0265	0.0182
	0.3051	0.032	0.1245	0.0296	0.0051	0.4682	0.0275	0.0195
	0.4142	0.0410	0.1585	0.0296	0.0051	0.4410	0.0280	0.0205
D-4	0.0993	0.0180	0.0704	0.0296	0.0107	0.5493	0.0366	0.0273
	0.1997	0.0244	0.0949	0.0296	0.0107	0.5493	0.0363	0.0264
	0.2853	0.0318	0.1234	0.0296	0.0107	0.4226	0.0406	0.0287
	0.4387	0.0395	0.1533	0.0296	0.0107	0.4359	0.0401	0.0273
	0.5844	0.0484	0.1880	0.0296	0.0107	0.2533	0.0525	0.0342
D-2	0.0400	0.0375	0.0429	0.0532	0.0025	0.1804	0.0357	0.0216
	0.0913	0.0692	0.0791	0.0532	0.0025	0.1662	0.0427	0.0284
	0.1575	0.1044	0.1192	0.0532	0.0025	0.1586	0.0500	0.0352
	0.1997	0.1236	0.1412	0.0532	0.0025	0.1601	0.0527	0.0380
	0.2266	0.1355	0.1548	0.0532	0.0025	0.0161	0.0546	0.0398
D-2	0.0507	0.0393	0.0449	0.0532	0.0047	0.2443	0.0378	0.0231
	0.0801	0.0568	0.0649	0.0532	0.0047	0.2110	0.0426	0.0275
	0.0998	0.0802	0.0917	0.0532	0.0047	0.1271	0.0412	0.0280
	0.1374	0.0869	0.0992	0.0532	0.0047	0.1883	0.0486	0.0334
	0.1752	0.1046	0.1196	0.0532	0.0047	0.1824	0.0513	0.0362
D-2	0.0964	0.0503	0.0574	0.0532	0.0091	0.4293	0.0395	0.0250
	0.1709	0.0833	0.0952	0.0532	0.0091	0.3207	0.0470	0.0322
	0.2310	0.1074	0.1227	0.0532	0.0091	0.2897	0.0510	0.0362
	0.3296	0.1429	0.1633	0.0532	0.0091	0.2716	0.0553	0.0407
D-1	0.0246	0.1575	0.0489	0.1005	0.0026	0.0511	0.0771	0.0477
	0.0422	0.2368	0.0735	0.1005	0.0026	0.0476	0.0895	0.0589
	0.0559	0.2896	0.0899	0.1005	0.0026	0.0477	0.0953	0.0646
	0.0722	0.3496	0.1085	0.1005	0.0026	0.0474	0.1017	0.0708
	0.1080	0.4673	0.1450	0.1005	0.0026	0.0481	0.1132	0.0819
D-1	0.0337	0.1548	0.0480	0.1005	0.0044	0.1371	0.0721	0.0446
	0.0522	0.2253	0.0699	0.1005	0.0044	0.1017	0.0832	0.0544
	0.0693	0.2859	0.0887	0.1005	0.0044	0.0870	0.0916	0.0620
	0.0973	0.3799	0.1179	0.1005	0.0044	0.0712	0.1011	0.0712
	0.1328	0.4793	0.1487	0.1005	0.0044	0.0734	0.1103	0.0801
D-1	0.0423	0.1509	0.0468	0.1005	0.0095	0.1535	0.0698	0.0428
	0.0613	0.2124	0.0659	0.1005	0.0095	0.1216	0.0807	0.0522
	0.0828	0.2788	0.0865	0.1005	0.0095	0.1031	0.0900	0.0607
	0.0958	0.3193	0.0991	0.1005	0.0095	0.0955	0.0960	0.0660
	0.1514	0.4697	0.1458	0.1005	0.0095	0.0843	0.1105	0.0800

TABLE II (Continued)

Spacing Ident.	Discharge (CFS)	dDB	$\frac{D}{b}$	$\frac{Nd}{b}$	S	$\frac{v^2}{gR}$	$\frac{n}{R^{1/6}}$	'n'
D-4	0.0356	0.0315	0.0408	0.0886	0.0022	0.1622	0.0343	0.0207
	0.0650	0.0483	0.0625	0.0886	0.0022	0.1630	0.0385	0.0247
	0.0890	0.0607	0.0786	0.0886	0.0022	0.1599	0.0412	0.0274
	0.1219	0.0761	0.0985	0.0886	0.0022	0.1588	0.0440	0.0302
	0.1748	0.0979	0.1267	0.0886	0.0022	0.1639	0.0477	0.0339
D-4	0.0317	0.0221	0.0286	0.0886	0.0045	0.3630	0.0306	0.0174
	0.0665	0.0393	0.0509	0.0886	0.0045	0.2974	0.0348	0.0216
	0.1302	0.0683	0.0884	0.0886	0.0045	0.2398	0.0421	0.0285
	0.1653	0.0820	0.1062	0.0886	0.0045	0.2313	0.0443	0.0308
	0.2278	0.1055	0.1367	0.0886	0.0045	0.2206	0.0486	0.0349
D-4	0.0863	0.0376	0.0487	0.0886	0.0095	0.5504	0.0353	0.0218
	0.1556	0.0624	0.0808	0.0886	0.0095	0.4179	0.0412	0.0275
	0.2310	0.0876	0.1135	0.0886	0.0095	0.3551	0.0460	0.0322
	0.3140	0.1137	0.1472	0.0886	0.0095	0.3216	0.0500	0.0363
	0.3964	0.1372	0.1777	0.0886	0.0095	0.3077	0.0527	0.0391
D-2	0.0205	0.1219	0.0464	0.1596	0.0023	0.0395	0.0812	0.0499
	0.0377	0.1904	0.0725	0.1596	0.0023	0.0398	0.0958	0.0630
	0.0541	0.2417	0.0921	0.1596	0.0023	0.0425	0.1015	0.0690
	0.0726	0.2950	0.1124	0.1596	0.0023	0.0420	0.1053	0.0736
	0.1005	0.3616	0.1377	0.1596	0.0023	0.0470	0.1081	0.0777
D-2	0.0205	0.0867	0.0330	0.1596	0.0045	0.1035	0.0601	0.0351
	0.0670	0.2295	0.0874	0.1596	0.0045	0.0697	0.0849	0.0574
	0.0801	0.2681	0.1021	0.1596	0.0045	0.0661	0.0949	0.0655
	0.0934	0.2938	0.1119	0.1596	0.0045	0.0675	0.0904	0.0632
	0.1282	0.3740	0.1424	0.1596	0.0045	0.0658	0.0995	0.0719
D-2	0.0279	0.0839	0.0320	0.1596	0.0096	0.1996	0.0597	0.0346
	0.0572	0.1609	0.0613	0.1596	0.0096	0.1279	0.0772	0.0494
	0.0897	0.2385	0.0908	0.1596	0.0096	0.1036	0.0889	0.0603
	0.1161	0.3015	0.1149	0.1596	0.0096	0.0911	0.0983	0.0690
	0.1438	0.3640	0.1386	0.1596	0.0096	0.0844	0.1064	0.0762
D-1	0.0134	0.4863	0.0503	0.3014	0.0044	0.0151	0.1901	0.1181
	0.0250	0.7837	0.0811	0.3014	0.0044	0.0134	0.2176	0.1453
	0.0304	0.9170	0.0949	0.3014	0.0044	0.0128	0.2325	0.1587
	0.0370	1.0700	0.1107	0.3014	0.0044	0.0126	0.2485	0.1734
	0.0476	1.2898	0.1334	0.3014	0.0044	0.0124	0.2601	0.1862
D-1	0.0218	0.5405	0.0559	0.3014	0.0097	0.0250	0.1763	0.1113
	0.0339	0.8189	0.0847	0.3014	0.0097	0.0190	0.2178	0.1464
	0.0412	0.9653	0.0999	0.3014	0.0097	0.0179	0.2308	0.1588
	0.0482	1.0825	0.1120	0.3014	0.0097	0.0178	0.2349	0.1642
	0.0593	1.3022	0.1347	0.3014	0.0097	0.0162	0.2530	0.1814

TABLE III
MANNING'S COEFFICIENT, DISCHARGE, AND RELATED PI-TERMS FOR EXPERIMENT
ON SQUARE GRID SPACING OF ROUGHNESS ELEMENTS

Spacing Ident.	Discharge (CFS)	dDB	$\frac{D}{b}$	$\frac{Nd}{b}$	s	$\frac{v^2}{gR}$	$\frac{n}{R^{1/6}}$	'n'
S-2	0.0572	0.0273	0.0541	0.0532	0.0025	0.1819	0.0288	0.0181
	0.1388	0.0507	0.1005	0.0532	0.0025	0.1772	0.0339	0.0233
	0.1932	0.0630	0.1241	0.0532	0.0025	0.1915	0.0357	0.0253
	0.2332	0.0707	0.1402	0.0532	0.0025	0.2001	0.0370	0.0267
	0.2850	0.0805	0.1596	0.0532	0.0025	0.2104	0.0380	0.0274
S-2	0.0583	0.0175	0.0347	0.0532	0.0050	0.6850	0.0225	0.0132
	0.1951	0.0529	0.1048	0.0532	0.0050	0.3113	0.0330	0.0228
	0.2321	0.0544	0.1077	0.0532	0.0050	0.4332	0.0262	0.0182
	0.2850	0.0669	0.1325	0.0532	0.0050	0.3487	0.0323	0.0231
	0.2939	0.0755	0.1496	0.0532	0.0050	0.2620	0.0389	0.0283
S-2	0.0610	0.0187	0.0370	0.0532	0.0107	0.8679	0.0342	0.0202
	0.1531	0.0349	0.0692	0.0532	0.0107	0.7117	0.0339	0.0221
	0.2321	0.0490	0.0971	0.0532	0.0107	0.5907	0.0364	0.0250
	0.328	0.0637	0.1262	0.0532	0.0107	0.4944	0.0386	0.0274
	0.4587	0.0865	0.1714	0.0532	0.0107	0.4409	0.0417	0.0309
S-1	0.0093	0.3256	0.0187	0.1005	0.0027	0.1111	0.0433	0.0231
	0.0289	0.7158	0.0412	0.1005	0.0027	0.1065	0.0473	0.0285
	0.0528	1.1231	0.0646	0.1005	0.0027	0.0986	0.0538	0.0348
	0.1057	1.8798	0.1080	0.1005	0.0027	0.0943	0.0647	0.0450
	0.1258	2.2726	0.1306	0.1005	0.0027	0.0798	0.0758	0.0541
S-1	0.0375	0.5787	0.0333	0.1005	0.0049	0.3276	0.0343	0.0200
	0.0973	1.4237	0.0818	0.1005	0.0049	0.1714	0.0535	0.0358
	0.1387	1.9378	0.1114	0.1005	0.0049	0.1503	0.0618	0.0432
	0.1692	2.2818	0.1311	0.1005	0.0049	0.1432	0.0663	0.0473
	0.1926	2.5138	0.1445	0.1005	0.0049	0.1427	0.0684	0.0495
S-1	0.0190	0.3414	0.0196	0.1005	0.0102	0.3972	0.0433	0.0232
	0.0472	0.9293	0.0534	0.1005	0.0102	0.1276	0.0758	0.0475
	0.1013	1.3063	0.0751	0.1005	0.0102	0.2188	0.0581	0.0384
	0.1670	2.0000	0.1149	0.1005	0.0102	0.1819	0.0673	0.0472
	0.2177	2.4901	0.1431	0.1005	0.0102	0.1700	0.0720	0.0521
S-1/2	0.0150	0.2628	0.0408	0.1950	0.0029	0.0325	0.0997	0.0600
	0.0256	0.3939	0.0612	0.1950	0.0029	0.0305	0.1140	0.0731
	0.0403	0.5514	0.0857	0.1950	0.0029	0.0295	0.1269	0.0854
	0.0481	0.6260	0.0973	0.1950	0.0029	0.0297	0.1324	0.0908
	0.0668	0.8044	0.1250	0.1950	0.0029	0.0287	0.1471	0.1044
S-1/2	0.0198	0.2974	0.0462	0.1950	0.0039	0.0424	0.1072	0.0658
	0.0340	0.4524	0.0703	0.1950	0.0039	0.0369	0.1207	0.0790
	0.0438	0.5509	0.0856	0.1950	0.0039	0.0354	0.1292	0.0871
	0.0592	0.6962	0.1082	0.1950	0.0039	0.0337	0.1407	0.0980
	0.0842	0.9107	0.1415	0.1950	0.0039	0.0330	0.1558	0.1124
S-1/2	0.0129	0.1326	0.0206	0.1950	0.0096	0.1668	0.0680	0.0367
	0.0391	0.3764	0.0585	0.1950	0.0096	0.0694	0.1066	0.0678
	0.0623	0.5733	0.0891	0.1950	0.0096	0.0547	0.1267	0.0858
	0.0760	0.6835	0.1062	0.1950	0.0096	0.0504	0.1359	0.0944
	0.0994	0.8658	0.1346	0.1950	0.0096	0.0458	0.1504	0.1079

TABLE III (Continued)

Spacing Ident.	Discharge (CFS)	dDB	$\frac{D}{b}$	$\frac{Nd}{b}$	s	$\frac{v^2}{gR}$	$\frac{n}{R^{1/6}}$	'n'
S-2	0.0298	0.075	0.0496	0.1596	0.0018	0.0629	0.0415	0.0257
	0.0516	0.0980	0.0648	0.1596	0.0018	0.0917	0.0491	0.0317
	0.0734	0.1226	0.0810	0.1596	0.0018	0.1100	0.0546	0.0365
	0.0902	0.1431	0.0946	0.1596	0.0018	0.1051	0.0580	0.0396
	0.1296	0.1847	0.1221	0.1596	0.0018	0.1069	0.0630	0.0445
S-2	0.0282	0.0445	0.0294	0.1596	0.0042	0.2691	0.0347	0.0197
	0.0890	0.1002	0.0662	0.1596	0.0042	0.2811	0.0408	0.0264
	0.1080	0.1195	0.0789	0.1596	0.0042	0.2511	0.0444	0.0295
	0.1467	0.1571	0.1038	0.1596	0.0042	0.2126	0.0509	0.0352
	0.2198	0.2234	0.1476	0.1596	0.0042	0.1781	0.0602	0.0437
S-2	0.0394	0.0445	0.0294	0.1596	0.0104	0.5075	0.0378	0.0216
	0.0775	0.0788	0.0521	0.1596	0.0104	0.3661	0.0447	0.0279
	0.1154	0.1123	0.0742	0.1596	0.0104	0.2916	0.0505	0.0333
	0.1792	0.1671	0.1104	0.1596	0.0104	0.2295	0.0589	0.0411
	0.2037	0.1879	0.1242	0.1596	0.0104	0.2144	0.0620	0.0439
S-1	0.0154	0.2602	0.0499	0.3014	0.0021	0.0198	0.1236	0.0768
	0.0286	0.4168	0.0799	0.3014	0.0021	0.0202	0.1602	0.1067
	0.0393	0.5204	0.0997	0.3014	0.0021	0.0191	0.1604	0.1104
	0.0467	0.5703	0.1092	0.3014	0.0021	0.0221	0.1647	0.1148
	0.0564	0.6581	0.1261	0.3014	0.0021	0.0181	0.1605	0.1139
S-1	0.0155	0.1780	0.0341	0.3014	0.0045	0.0587	0.0860	0.0502
	0.0386	0.4200	0.0805	0.3014	0.0045	0.0328	0.1389	0.0927
	0.0468	0.4864	0.0932	0.3014	0.0045	0.0324	0.1464	0.0998
	0.0623	0.5916	0.1133	0.3014	0.0045	0.0335	0.1526	0.1068
	0.0714	0.6739	0.1291	0.3014	0.0045	0.0258	0.1525	0.1086
S-1	0.0336	0.2930	0.0561	0.3014	0.0104	0.0571	0.1204	0.0762
	0.0484	0.4002	0.0767	0.3014	0.0104	0.0495	0.1339	0.0889
	0.0604	0.4793	0.0918	0.3014	0.0104	0.0461	0.1402	0.0954
	0.0783	0.5869	0.1124	0.3014	0.0104	0.0442	0.1466	0.1027
	0.1075	0.7577	0.1452	0.3014	0.0104	0.0419	0.1583	0.1147
S-1/2	0.0065	0.9375	0.0486	0.5850	0.0020	0.0070	0.3098	0.1920
	0.0114	0.4157	0.0733	0.5850	0.0020	0.0066	0.3578	0.2359
	0.0167	0.8720	0.0970	0.5850	0.0020	0.0064	0.4023	0.2759
	0.0236	2.4336	0.1261	0.5850	0.0020	0.0066	0.4556	0.3239
	0.0269	2.6354	0.1365	0.5850	0.0020	0.0070	0.4636	0.3330
S-1/2	0.0075	1.0983	0.0569	0.5850	0.0047	0.0028	0.3357	0.2128
	0.0202	1.9320	0.1001	0.5850	0.0047	0.0072	0.4020	0.2771
	0.0146	1.4698	0.0761	0.5850	0.0047	0.0078	0.3534	0.2343
	0.0299	2.6427	0.1369	0.5850	0.0047	0.0071	0.4619	0.3322
	0.0350	2.9967	0.1552	0.5850	0.0047	0.0067	0.4872	0.3560
S-1/2	0.0171	1.2855	0.0666	0.5850	0.0101	0.0119	0.3162	0.2056
	0.0247	1.8179	0.0942	0.5850	0.0101	0.0104	0.3744	0.2560
	0.0385	2.7261	0.1412	0.5850	0.0101	0.0089	0.4537	0.3278
	0.0417	2.8884	0.1496	0.5850	0.0101	0.0089	0.4582	0.3335
	0.0321	2.2850	0.1184	0.5850	0.0101	0.0098	0.4127	0.2912

$$\text{Cubic: } Y = C_1 + C_2 X_1 + C_3 X_1^2 + C_4 X_1^3 + C_5 X_2 + C_6 X_2^2 + C_7 X_2^3 + C_8 X_3 +$$

$$C_9 X_3^2 + C_{10} X_3^3 + C_{11} X_4 + C_{12} X_4^2 + C_{13} X_4^3 + C_{14} X_5 + C_{15} X_5^2 +$$

$$C_{16} X_5^3 \quad (5-8)$$

$$\text{where } Y = \pi_1$$

$$X_4 = \pi_5$$

$$X_1 = \pi_2$$

$$X_5 = \pi_6$$

$$X_2 = \pi_3$$

C = Experimental Coefficient

$$X_3 = \pi_4$$

From another perspective, an exponential model relating the six pi-terms under study was built with the equation

$$\pi_1 = A \pi_2^B \pi_3^C \pi_4^D \pi_5^E \pi_6^F \quad (5-9)$$

where A, B, C, D, E, F are experimental coefficients.

Regression analysis using logarithmic transformations uncovered the relationship between the terms as shown in Table IV.

Order of Experimental Analysis

One hundred seventy four experiments were analyzed. Six pi-terms were calculated for further analysis in each experiment. Some criteria were used in breaking the analyses down into four major groups. The first criteria was the pattern of spacing; i.e., Diagonal or Square grid system. The second criteria was the size of peg diameter. Thus,

TABLE IV

MULTIVARIATE EXPONENTIAL RELATIONSHIP FOR $\frac{n}{R^{1/6}}$ *

Size and Pattern of Roughness Element	Correlation Coefficient (R)	Standard Deviation (S)	Exponential Model Equations
D - $\frac{3}{32}$	0.947	0.0092	$\pi_1 = 10^{-23} \times 1.05 \pi_2^{8.96} \pi_3^{-8.80} \pi_4^{-17.86} \pi_5^{0.218} \pi_6^{-0.192}$
D - $\frac{9}{32}$	0.999	0.0037	$\pi_1 = 30.8 \pi_2^{-0.787} \pi_3^{1.051} \pi_4^{2.448} \pi_5^{0.097} \pi_6^{-0.221}$
S - $\frac{3}{32}$	0.990	0.0057	$\pi_1 = 0.562 \pi_2^{-0.00005} \pi_3^{0.170} \pi_4^{2.467} \pi_5^{0.267} \pi_6^{-0.346}$
S - $\frac{9}{32}$	0.999	0.0079	$\pi_1 = 1.35 \pi_2^{0.009} \pi_3^{0.351} \pi_4^{1.353} \pi_5^{-0.0002} \pi_6^{-0.064}$
D - $\frac{3}{32}$ & D - $\frac{9}{32}$	0.991	0.0082	$\pi_1 = 0.172 \pi_2^{0.282} \pi_3^{-0.084} \pi_4^{0.033} \pi_5^{0.208} \pi_6^{-0.276}$
S - $\frac{3}{32}$ & S - $\frac{9}{32}$	0.970	0.032	$\pi_1 = 0.26 \pi_2^{0.041} \pi_3^{0.158} \pi_4^{0.266} \pi_5^{0.248} \pi_6^{-0.439}$
Diagonal and Square all Combined	0.968	0.027	$\pi_1 = 0.25 \pi_2^{0.035} \pi_3^{0.141} \pi_4^{0.198} \pi_5^{0.273} \pi_6^{-0.454}$

* Equation (5-9)

for each size of peg, all the diagonal grids were grouped together and all the square grid systems were in another group. In each group all the pi-terms were arranged in increasing order of discharge, test slope, and density of spacing as identified below.

Identification Technique for Peg Size,
Arrangement and Spacing

Pattern of Element Placement	Peg Size Symbol	Longitudinal Spacing (inches)	Transverse Spacing (inches)	Spacing Symbol
Diagonal	$D - \frac{3}{32}$	4	4	D - 4
Diagonal	$D - \frac{9}{32}$	2	2	D - 2
Diagonal		1	1	D - 1
Square	$S - \frac{3}{32}$	2	2	S - 2
Square	$S - \frac{9}{32}$	1	1	S - 1
Square		$\frac{1}{2}$	$\frac{1}{2}$	S - $\frac{1}{2}$

Multivariable polynomial programs in linear, quadratic and cubic forms were used to analyze each group experiment. Further combinations of all diagonal-grid and all square-grid experiments irrespective of sizes were respectively classified into two groups. Finally all the 174 experimental results were combined into a single group. Prediction equations were established for the dimensionless roughness coefficient. The results including correlation coefficients and standard deviations are shown in Tables V, VI and VII. A summary of

TABLE V

EXPERIMENTAL COEFFICIENTS, CORRELATION COEFFICIENT (R), AND STANDARD DEVIATION (S) OF MULTIVARIABLE LINEAR EQUATIONS FOR COMPUTING DIMENSIONLESS RESISTANCE COEFFICIENTS *

Exp. Coeff.	Size and Pattern of Spacing of Roughness Elements						Diagonal and Square all Combined
	$D - \frac{3}{32}$	$D - \frac{9}{32}$	$S - \frac{3}{32}$	$S - \frac{9}{32}$	$D - \frac{3}{32}$ & $D - \frac{9}{32}$	$S - \frac{3}{32}$ & $S - \frac{9}{32}$	
	R=0.989 S=0.0043	R=0.998 S=0.0049	R=0.970 S=0.0101	R=0.997 S=0.0124	R=0.991 S=0.0081	R=0.981 S=0.025	
C_1	0.0221	-0.0295	-0.0415	-0.0883	0.0269	-0.0730	-0.0358
C_2	0.1279	0.0818	0.0013	0.0567	0.1392	0.0301	0.0260
C_3	-0.0109	0.1422	0.2881	0.3483	-0.0278	0.3500	0.3100
C_4	0.2815	0.5836	0.7218	0.6087	0.2185	0.6529	0.5866
C_5	1.1176	-1.4695	-0.2112	-2.4500	0.5781	-1.6628	-0.2807
C_6	-0.0228	0.0309	0.0183	0.0835	-0.0261	0.0706	0.0065

* Equation (5-6)

TABLE VI

EXPERIMENTAL COEFFICIENTS, CORRELATION COEFFICIENT (R), AND STANDARD DEVIATION (S)
OF MULTIVARIABLE QUADRATIC EQUATIONS FOR COMPUTING
DIMENSIONLESS RESISTANCE COEFFICIENTS *

Exp. Coeff.	Size and Pattern of Spacing of Roughness Elements						Diagonal and Square all Combined
	D - $\frac{3}{32}$	D - $\frac{9}{32}$	S - $\frac{3}{32}$	S - $\frac{9}{32}$	D- $\frac{3}{32}$ & D- $\frac{9}{32}$	S- $\frac{3}{32}$ & S- $\frac{9}{32}$	
	R=0.992 S=0.0036	R=0.999 S=0.0039	R=0.987 S=0.0068	R=0.999 S=0.0082	R=0.997 S=0.0051	R=0.987 S=0.0207	
C ₁	0.0460	-0.0327	-0.0213	-0.1307	0.0506	0.0351	0.0219
C ₂	0.2061	0.1166	0.0202	-0.0200	0.1845	-0.0149	-0.0051
C ₃	-0.1208	-0.0202	-0.0095	0.0218	-0.0492	0.0126	0.0085
C ₄	-0.0135	0.3448	0.4976	1.5070	0.0099	0.2014	0.4465
C ₅	-0.1804	-1.1988	-0.9727	-5.7272	-0.3294	0.4948	-0.9892
C ₆	-0.1680	0.5870	0.5702	0.7339	-0.0968	0.1060	0.0819
C ₇	2.1129	-0.0328	-0.1732	-0.0472	0.9096	0.6973	0.6986
C ₈	-1.4654	-7.3500	1.2294	-8.0537	-1.0595	5.0530	12.7423
C ₉	210.7	443.22	-36.1448	464.6	142.06	-322.54	-834.8
C ₁₀	-0.0596	0.0807	-0.1450	0.0051	-0.0888	-0.2985	-0.3520
C ₁₁	0.0532	-0.0484	0.1760	0.1884	0.0935	0.3337	0.3892

* Equation (5-7)

TABLE VII

EXPERIMENTAL COEFFICIENTS (C), CORRELATION COEFFICIENT (R), AND STANDARD DEVIATION (S) OF
MULTIVARIABLE CUBIC EQUATIONS FOR COMPUTING DIMENSIONLESS RESISTANCE COEFFICIENTS *

Exp.	Size and Pattern of Spacing of Roughness Elements						Diagonal and Square all Combined
	$D - \frac{3}{32}$	$D - \frac{9}{32}$	$S - \frac{3}{32}$	$S - \frac{9}{32}$	$D - \frac{3}{32}$ & $D - \frac{9}{32}$	$S - \frac{3}{32}$ & $S - \frac{9}{32}$	
	R=0.996	R=0.998	R=0.996	R=0.996	R=0.998	R=0.992	
Coeff.	S=0.0024	S=0.0045	S=0.0039	S=0.014	S=0.0042	S=0.016	S=0.019
C ₁	0.0120	-0.3370	0.0993	0.0696	0.0162	0.0640	0.1022
C ₂	0.4858	0.0471	0.1603	-0.0765	0.2409	0.0662	0.0544
C ₃	-0.9209	0.0610	-0.1038	0.0591	-0.1562	-0.0711	-0.0503
C ₄	0.8068	-0.0318	0.0208	-0.0085	0.0543	0.0207	0.0149
C ₅	-0.1101	1.1063	-1.6998	2.0752	0.3565	-1.0449	-0.3225
C ₆	-0.4878	-8.7474	18.8610	-12.591	-4.4449	18.2425	7.7208
C ₇	1.9014	24.9180	-61.3042	33.615	13.4663	-70.5781	-31.8799
C ₈	-0.0737	1.4635	-0.5407	1.5641	-0.0350	0.5041	-0.1872
C ₉	-3.8508	-4.8632	-12.0362	-0.6543	0.4180	-1.6460	1.5112
C ₁₀	32.00	8.0944	69.6445	-0.4876	1.0551	2.8352	-0.8028
C ₁₁	18.608	182.20	40.2839	-314.5	13.336	-3.609	-9.982
C ₁₂	-3857.0	-40684.0	-7037.0	66896.0	-2827.	1218.0	3415.6
C ₁₃	230972.	-2507281.0	379089.0	-3921188	171624.	-80153.	231193.0
C ₁₄	-0.0393	-0.0474	-0.3339	0.3230	-0.12493	-0.6013	-0.5964
C ₁₅	0.1747	0.5072	0.5834	0.4438	0.3827	1.4065	1.2957
C ₁₆	-0.2234	-0.5960	-0.3302	-1.1000	-0.3854	-0.8995	-0.8226

* Equation (5-8)

correlation coefficient (R), and standard deviation (S) of multivariate equations for predicting dimensionless resistance coefficient is given in Table VIII.

General Discussion on Prediction Equations

In general, it can be seen from Table VIII that correlation coefficient between the observed and calculated values of $\frac{n}{R^{1/6}}$ is very high. This evidence may strongly prove the dependence of roughness coefficient on the size, spacing, and pattern of roughness elements in a water conveyance channel. The values of correlation coefficient also increases with the degree of polynomial used. It is sometimes questionable whether a polynomial of the degree greater than two should be considered as a criteria since the coefficient R hardly increases. In fact, in some cases, there is a decrease in R in polynomial of the third degree. However, the use of the second degree polynomial is probably justified by a considerable improvement in the standard deviations. In this particular experiment, standard deviation was a better criteria rather than coefficient of correlation R. Generally, the percentage difference between calculated and observed values of Y in Equations (5-6), (5-7) and (5-8) was below 6 per cent, though a few extreme cases of 11 per cent have been recorded.

Comparing the two patterns studied, the extremely high correlation coefficients associated with both independent systems of diagonal-grid and square-grid degenerated as both patterns were combined either with respect to size or exclusive of size and pattern. It is worthy of note that the exponential multivariable model gave smaller values of standard deviation only for the square grid system. There was no strong evidence

TABLE VIII

SUMMARY OF CORRELATION COEFFICIENT (R) AND STANDARD DEVIATION (S) OF MULTIVARIABLE EQUATIONS FOR PREDICTING DIMENSIONLESS RESISTANCE COEFFICIENTS

Pattern of Roughness Elements	Exponential				Linear				Quadratic				Cubic			
	$\frac{3}{32}$ " diam.		$\frac{9}{32}$ " diam.		$\frac{3}{32}$ " diam.		$\frac{9}{32}$ " diam.		$\frac{3}{32}$ " diam.		$\frac{9}{32}$ " diam.		$\frac{3}{32}$ " diam.		$\frac{9}{32}$ " diam.	
	R	S	R	S	R	S	R	S	R	S	R	S	R	S	R	S
Diagonal	0.947	0.0092	0.999	0.0037	0.989	0.0043	0.998	0.0049	0.992	0.0036	0.999	0.0039	0.996	0.0024	0.998	0.0045
Square	0.990	0.0057	0.999	0.0079	0.970	0.0101	0.997	0.0124	0.987	0.0068	0.999	0.0082	0.996	0.0039	0.996	0.014
Diagonal for Combined Sizes	R = 0.991 S = 0.0082				R = 0.991 S = 0.0081				R = 0.997 S = 0.0051				R = 0.998 S = 0.0042			
Square for Combined Sizes	R = 0.970 S = 0.032				R = 0.981 S = 0.025				R = 0.987 S = 0.0207				R = 0.992 S = 0.016			
Combined Diagonal and Square	R = 0.968 S = 0.026				R = 0.967 S = 0.027				R = 0.979 S = 0.021				R = 0.983 S = 0.019			

to believe that the exponential model was better than the linear relationship model.

Further examination of the results of coefficients in Tables IV through VII revealed the following relationships between the dependent and independent pi-terms:

1. The positive effect of the coefficient of the term dDB in every degree of polynomial confirmed that size increase as well as increased density of spacing caused the retardance to flow of water in open channels to increase.
2. The resistance to flow increased as the depth of flow increased in the term $\frac{D}{b}$. It is important to recognize that the validity of this holds provided the whole length of the roughness elements remained unsubmerged as indicated in the previous assumption.
3. For all practical purposes, with the same size of element, slope of the channel, and discharge, the resistance to flow increased commensurably with the increase of $\frac{Nd}{b}$.
4. The term $\frac{n}{R^{1/6}}$ generally decreased slightly with increase in slope.
5. The resistance coefficient increased with a decrease in Froude number.

CHAPTER VI

SUMMARY AND CONCLUSIONS

Summary

Gradually-varied flow experiments were conducted in a 1.32-foot wide and 24-foot long test section of a WF steel beam channel. The bottom of the channel was lined with aluminum sheet material which was fitted with round aluminum pegs of sizes 3/32-inch and 9/32-inch diameters. The pegs which served as roughness elements were placed in the channel bed at definite longitudinal and transverse patterns and spacings. Under the bare-channel lining condition a maximum flow of 0.885 c.f.s. was allowed into the channel. Test slopes for the adjustable slope channel were restricted to approximate values of 0.0025, 0.0050, and 0.010. Density of roughness elements was progressively increased transversely from four inches to one-half inch.

The objective of this study was to determine the relationship of Manning's resistance coefficient to size of roughness elements, pattern of arrangement, density of spacing, slope, and discharge in a smooth artificial channel using dimensional analysis and gradually-varied flow. Multivariable polynomial equations of first, second, and third degree, and an exponential model were used to analyze the data for a selected group of dimensionless terms. Correlation coefficient (R) and standard deviation (S) were established from a least square linear regression equation. The effect of variable parameters was

critically discussed.

Conclusions

The following conclusions are based on the analysis and interpretation of the experimental results.

1. An increase in size or density of roughness elements increased the resistance to flow in open channel.

2. A Diagonal-grid pattern of roughness elements offered less resistance to flow in the open channel than a Square-grid pattern.

3. Resistance to flow in the open channel slightly decreased with increase in slope.

4. Resistance to flow decreased with increase in discharge under smooth channel condition but it increased with discharge when channel was fitted with roughness elements.

5. A linear model equation $Y = C_1 + C_2X_1 + C_3X_2 + C_4X_3 + C_5X_4 + C_6X_5$ and an exponential model $Y = AX_1^B X_2^C X_3^D X_4^E X_5^F$ gave comparable standard deviations. A quadratic model $Y = C_1 + C_2X_1 + C_3X_1^2 + C_4X_2 + C_5X_2^2 + C_6X_3 + C_7X_3^2 + C_8X_4 + C_9X_4^2 + C_{10}X_5 + C_{11}X_5^2$ gave improved estimates, but it was more complex to calculate. A cubic model $Y = C_1 + C_2X_1 + C_3X_1^2 + C_4X_1^3 + C_5X_2 + C_6X_2^2 + C_7X_2^3 + C_8X_3 + C_9X_3^2 + C_{10}X_3^3 + C_{11}X_4 + C_{12}X_4^2 + C_{13}X_4^3 + C_{14}X_5 + C_{15}X_5^2 + C_{16}X_5^3$ sometimes gave slightly improved estimates but it was not recommended because of its complexity.

Suggestions for Future Study

Based on the results of this study, the following research is suggested to improve the methods for predicting the degree of resistance to flow in open channels.

1. In most of the experiments, surface waves and standing waves were major problems at high discharges and density of roughness elements. An extension of the hydraulic phenomena encountered in this study might include the effect of surface wave velocities in future study.

2. A study of steady state spatially-varied flow profiles of these tests and other tests with different roughness elements is needed.

3. There is probably a marked relationship between the effect of the roughness of the channel and that of different roughness elements. A contribution of each to the total resistance to flow should be further examined.

A study of the effect of different roughness elements and combinations of these elements at high slopes up to 5 per cent should be studied to completely understand the phenomena under gradually-varied flow.

A SELECTED BIBLIOGRAPHY

1. Boyer, M. C. "Estimating the Roughness Coefficient From an Average Bed Roughness in Open Channel." Transactions of the American Geophysical Union, (December, 1954), p. 957.
2. Chow, Ven Te. "A Note on Manning's Formula." Transactions of the American Geophysical Union, Vol. 36, 4 (August, 1955), p. 668.
3. Chow, Ven Te. Open Channel Hydraulics. New York: McGraw-Hill Book Company, Inc., 1959.
4. Einstein, H. A. and R. B. Banks. "Fluid Resistance of Composite Roughness." Transactions of the American Geophysical Union, Vol. 31 (August, 1950), pp. 603-10.
5. Fang, Benjamin P. "Manning Retardance Coefficients for Upright Stems of Vegetation in Channels with Moderate Flow Velocities." M. S. Thesis, Oklahoma State University, Stillwater, Oklahoma, May, 1960.
6. Henderson, F. M. Open Channel Flow. New York: The MacMillan Company, 1966.
7. Murphy, C. E. Similitude in Engineering. New York: The Ronald Press Company, 1950.
8. Olson III, E. G. "Hydrodynamics of Unsteady Open-Channel Fluid Flow Over a Porous Bed Having a Variable Infiltration Rate." Ph.D. Dissertation, College of Engineering, Utah State University, Logan, Utah, June, 1965.
9. Johnson, J. W. "Rectangular Artificial Roughness in Open Channels." Transactions of the American Geophysical Union, Vol. 25 (1944), p. 906.
10. Powell, Ralph W. "Flow in a Channel of Definite Roughness." Transactions of the American Society of Civil Engineers, III (1946), pp. 531-66.
11. Powell, Ralph W. "Resistance to Flow in Rough Channels." Transactions of the American Geophysical Union, (August, 1950), pp. 575-82.

12. Rand, W. "Discussion of Artificial Roughness Standard for Open Channels." Transactions of the American Geophysical Union, Vol. 35 (August, 1954), pp. 649-51.
13. Ree, W. O. "Some Experiments on Shallow Flows Over a Grassed Slope." Transactions of the American Geophysical Union (1939).
14. Ree, W. O. "The Use of Grass in Waterways." Proceedings of the Sixth International Grassland Congress.
15. Ree, W. O. "Retardance Coefficient for Row Crops in Diversion Terraces." Transactions of the American Society of Agricultural Engineers, Vol. 1, No. 1 (1958), pp. 78-80.
16. Robertson, A. F., A. K. Turner, F. R. Crow and W. O. Ree. "Run-off From Impervious Surfaces Under Conditions of Simulated Rainfall." Transactions of the American Society of Agricultural Engineers, Vol. 9, No. 3 (1966), pp. 343-46.
17. Robinson, A. R. "Artificial Roughness in Open Channels." M. S. Thesis, Colorado A & M, Fort Collins, Colorado, 1950.
18. Robinson, A. R. and M. L. Albertson. "Artificial Roughness Standard for Open Channels." Transactions of the American Society of Civil Engineers, Vol. 33, No. 6 (December, 1952).
19. Rodman, Paul K. "Steady State Increasing Spatially-Varied Flow Over a Simulated Vegetated Surface." M. S. Thesis, Oklahoma State University, Stillwater, Oklahoma, August, 1969.
20. Rouse, H. Elementary Mechanics of Fluids. New York: John Wiley and Sons, Inc., 1946.
21. Rouse, H. "Analysis of Open Channel Resistance." Transactions of the American Society of Civil Engineers, Vol. 131 (1966) p. 851.
22. Sayre, W. W. "Artificial Roughness Patterns in Open Channels." M. S. Thesis, Colorado State University, Fort Collin, Colorado, 1957.
23. Sayre, W. W. and M. L. Albertson. "Roughness Spacing in Rigid Open Channels." American Society of Civil Engineers Proc., Vol. 87 [Hy. 3, No. 2823] (May, 1961), pp. 121-50.
24. Stillwater Outdoor Hydraulic Laboratory. "Handbook of Channel Design for Soil and Water Conservation." United States Department of Agriculture Soil Conservation Service. SCS-TP-61. June, 1954.
25. Scobey, F. C. "Flow of Water in Irrigation and Similar Canals." Technical Bulletin No. 652 United States Department of Agriculture, 1939.

26. Woodward, S. M. and C. J. Posey. Steady Flow in Open Channels.
New York: John Wiley and Sons, Inc., 1958.
27. Woody, L. Cowan. "Estimating Hydraulic Roughness Coefficients."
Agricultural Engineering, Vol. 37, No. 7 (July, 1956),
pp. 473-75.

APPENDICES

APPENDIX A

EXPERIMENTAL DATA FOR THE $\frac{3}{32}$ -INCH DIAMETER ROUGHNESS ELEMENTS

Spacing Ident.	Slope	Temperature °F	Discharge (cfs)	Station Depths of Flow (Ft)				
				0 + 00	0 + 05	0 + 10	0 + 15	0 + 20
D-4	0.0022	80.0	0.1230	0.1000	0.1020	0.0970	0.0970	0.0990
		80.5	0.1857	0.1420	0.1430	0.1380	0.1370	0.1360
		81.0	0.2325	0.1670	0.1680	0.1620	0.1590	0.1560
		81.0	0.2962	0.2010	0.2000	0.1900	0.1870	0.1810
		81.0	0.3229	0.2130	0.2100	0.2010	0.1950	0.1870
D-4	0.0051	78.0	0.0295	0.0310	0.0315	0.0290	0.0290	0.0345
		78.0	0.1297	0.0810	0.0830	0.0780	0.0810	0.0850
		78.0	0.2320	0.1320	0.1340	0.1290	0.1330	0.1350
		80.0	0.3051	0.1645	0.1660	0.1615	0.1645	0.1650
		81.0	0.4142	0.2045	0.2120	0.2095	0.2110	0.2090
D-4	0.0107	78.5	0.0993	0.0930	0.0955	0.0900	0.0870	0.0990
		79.0	0.1997	0.1280	0.1270	0.1220	0.1170	0.1320
		80.0	0.2853	0.1655	0.1660	0.1590	0.1530	0.1710
		81.0	0.4387	0.2040	0.2030	0.1970	0.2010	0.2070
		81.5	0.5844	0.2540	0.2480	0.2430	0.2480	0.2480
S-2	0.0025	81.0	0.0572	0.0645	0.0705	0.0700	0.0745	0.0775
		81.5	0.1388	0.1345	0.1365	0.1325	0.1315	0.1285
		81.5	0.1932	0.1705	0.1725	0.1640	0.1605	0.1515
		81.5	0.2332	0.1965	0.1955	0.1860	0.1795	0.1675
		82.0	0.2850	0.2255	0.2245	0.2130	0.2035	0.1865
S-2	0.0050	82.0	0.0583	0.0430	0.0460	0.0450	0.0450	0.0500
		82.5	0.1951	0.1350	0.1385	0.1360	0.1400	0.1420
		82.0	0.2321	0.1170	0.1370	0.1490	0.1510	0.1570
		82.5	0.2850	0.1890	0.1590	0.1725	0.1770	0.1770
		82.0	0.2939	0.2010	0.2020	0.1950	0.2030	0.1860

APPENDIX A (Continued)

Spacing Ident.	Slope	Temperature °F	Discharge (cfs)	Station Depths of Flow (Ft)				
				0 + 00	0 + 05	0 + 10	0 + 15	0 + 20
S-2	0.0107	83.0	0.0610	0.0320	0.0420	0.0500	0.0560	0.0640
		83.0	0.1531	0.0705	0.0840	0.0940	0.1010	0.1070
		83.5	0.2321	0.1030	0.1240	0.1330	0.1405	0.1400
		84.0	0.3140	0.1430	0.1640	0.1720	0.1770	0.1770
		84.5	0.4587	0.2090	0.2300	0.2350	0.2370	0.2200
D-2	0.0025	82.0	0.0400	0.0605	0.0595	0.0575	0.0585	0.0470
		82.0	0.0913	0.1165	0.1125	0.1075	0.1035	0.0820
		82.0	0.1575	0.1805	0.1725	0.1625	0.1515	0.1200
		82.0	0.1997	0.2155	0.2055	0.1925	0.1775	0.1410
		82.0	0.2266	0.2375	0.2255	0.2110	0.1945	0.1530
D-2	0.0047	81.5	0.0507	0.0550	0.0615	0.0600	0.0625	0.0570
		82.0	0.0801	0.0850	0.0905	0.0880	0.0885	0.0760
		82.0	0.0998	0.1030	0.1165	0.1130	0.1315	0.1410
		82.0	0.1374	0.1380	0.1415	0.1350	0.1305	0.1100
		82.0	0.1752	0.1700	0.1705	0.1620	0.1555	0.1310
D-2	0.0091	79.5	0.0964	0.0730	0.0770	0.0790	0.0790	0.0710
		80.0	0.1709	0.1250	0.1310	0.1320	0.1290	0.1110
		80.0	0.2310	0.1660	0.1710	0.1710	0.1640	0.1380
		81.5	0.3296	0.2280	0.2310	0.2270	0.2150	0.1770
S-1	0.0027	78.0	0.0093	0.0225	0.0255	0.0275	0.0260	0.0220
		78.0	0.0289	0.0555	0.0575	0.0580	0.0555	0.0450
		78.0	0.0528	0.0915	0.0925	0.0905	0.0835	0.0680
		78.0	0.1057	0.1615	0.1575	0.1495	0.1355	0.1090
		78.0	0.1258	0.1975	0.1915	0.1815	0.1625	0.1290

APPENDIX A (Continued)

Spacing Ident.	Slope	Temperature °F	Discharge (cfs)	Station Depths of Flow (Ft)				
				0 + 00	0 + 05	0 + 10	0 + 15	0 + 20
S-1	0.0049	77.5	0.0375	0.0450	0.0475	0.0450	0.0440	0.0380
		77.0	0.0973	0.1190	0.1185	0.1125	0.1050	0.0850
		77.0	0.1387	0.1660	0.1635	0.1540	0.1405	0.1110
		77.5	0.1692	0.1980	0.1935	0.1810	0.1640	0.1290
		78.0	0.1926	0.2200	0.2135	0.1990	0.1800	0.1410
S-1	0.0102	77.0	0.0190	0.0245	0.0245	0.0265	0.0295	0.0245
		77.0	0.0472	0.0665	0.0715	0.0715	0.0765	0.0665
		77.0	0.1013	0.0985	0.1015	0.1005	0.1035	0.0915
		77.0	0.1670	0.1595	0.1595	0.1555	0.1545	0.1295
		77.5	0.2177	0.2015	0.2015	0.1955	0.1895	0.1565
D-1	0.0026	78.0	0.0246	0.0750	0.0735	0.0680	0.0555	0.0505
		78.0	0.0422	0.1140	0.1095	0.1010	0.0895	0.0710
		79.0	0.0559	0.1410	0.1345	0.1230	0.1090	0.0855
		79.0	0.0722	0.1710	0.1635	0.1490	0.1310	0.1015
		80.0	0.1080	0.2320	0.2195	0.1990	0.1740	0.1325
D-1	0.0044	80.0	0.0337	0.0790	0.0765	0.0675	0.0560	0.0380
		80.0	0.0522	0.1120	0.1095	0.0990	0.0830	0.0580
		81.0	0.0693	0.1425	0.1375	0.1240	0.1060	0.0755
		81.5	0.0973	0.1860	0.1815	0.1640	0.1405	0.1060
		82.0	0.1328	0.2390	0.2300	0.2080	0.1775	0.1270
D-1	0.0095	79.5	0.0423	0.0665	0.0660	0.0635	0.0590	0.0540
		80.0	0.0613	0.0945	0.0940	0.0885	0.0850	0.0730
		80.0	0.0828	0.1235	0.1240	0.1185	0.1120	0.0930
		79.0	0.0958	0.1445	0.1420	0.1365	0.1270	0.1040
		79.0	0.1514	0.2185	0.2130	0.2015	0.1840	0.1450

APPENDIX A (Continued)

Spacing Ident.	Slope	Temperature °F	Discharge (cfs)	Station Depths of Flow (Ft)				
				0 + 00	0 + 05	0 + 10	0 + 15	0 + 20
S- $\frac{1}{2}$	0.0029	77.0	0.0150	0.0605	0.0605	0.0555	0.0535	0.0395
		77.0	0.0256	0.0940	0.0920	0.0835	0.0775	0.0570
		77.0	0.0403	0.1335	0.1295	0.1175	0.1070	0.0780
		77.0	0.0481	0.1530	0.1475	0.1335	0.1205	0.0875
		78.0	0.0668	0.1995	0.1895	0.1715	0.1535	0.1110
S- $\frac{1}{2}$	0.0039	77.0	0.0198	0.0690	0.0710	0.0640	0.0590	0.0420
		77.0	0.0340	0.1060	0.1080	0.0970	0.0890	0.0640
		77.0	0.0438	0.1310	0.1310	0.1190	0.1070	0.0770
		77.5	0.0592	0.1680	0.1660	0.1500	0.1340	0.0960
		77.5	0.0842	0.2240	0.2180	0.1960	0.1730	0.1230
S- $\frac{1}{2}$	0.0096	78.5	0.0129	0.0220	0.0310	0.0290	0.0270	0.0270
		78.5	0.0391	0.0800	0.0830	0.0810	0.0770	0.0650
		79.0	0.0623	0.1260	0.1290	0.1240	0.1160	0.0930
		79.0	0.0760	0.1520	0.1550	0.1490	0.1370	0.1080
		79.0	0.0994	0.1990	0.1970	0.1890	0.1710	0.1320

APPENDIX B

EXPERIMENTAL DATA FOR THE $\frac{9}{32}$ -INCH DIAMETER ROUGHNESS ELEMENTS

Spacing Ident.	Slope	Temperature °F	Discharge (cfs)	Station Depths of Flow (Ft)				
				0 + 00	0 + 05	0 + 10	0 + 15	0 + 20
D-4	0.0022	75.0	0.0356	0.0535	0.0575	0.0575	0.0545	0.0465
		75.0	0.0650	0.0885	0.0895	0.0875	0.0805	0.0665
		75.0	0.0890	0.1135	0.1135	0.1085	0.1005	0.0825
		75.0	0.1219	0.1445	0.1425	0.1360	0.1245	0.1025
		75.0	0.1748	0.1895	0.1855	0.1745	0.1585	0.1285
D-4	0.0045	75.0	0.0317	0.0405	0.0400	0.0385	0.0370	0.0330
		75.0	0.0665	0.0730	0.0700	0.0685	0.0665	0.0580
		75.0	0.1302	0.1290	0.1240	0.1205	0.1150	0.0950
		75.0	0.1653	0.1560	0.1500	0.1450	0.1370	0.1130
		75.0	0.2278	0.2040	0.1960	0.1865	0.1735	0.1420
D-4	0.0095	74.0	0.0863	0.0640	0.0660	0.0655	0.0640	0.0620
		74.0	0.1556	0.1070	0.1100	0.1090	0.1080	0.0990
		74.0	0.2310	0.1550	0.1570	0.1590	0.1500	0.1330
		75.0	0.3140	0.2060	0.2060	0.2005	0.1920	0.1670
		76.0	0.3964	0.2520	0.2510	0.2420	0.2300	0.1980
S-2	0.0018	74.5	0.0298	0.0610	0.0645	0.0660	0.0660	0.0695
		74.5	0.0516	0.0930	0.0945	0.0900	0.0775	0.0725
		74.5	0.0734	0.1220	0.1215	0.1150	0.0990	0.0770
		74.5	0.0902	0.1440	0.1415	0.1320	0.1150	0.0915
		74.5	0.1296	0.1880	0.1835	0.1700	0.1475	0.1165
S-2	0.0042	74.0	0.0282	0.0425	0.0420	0.0385	0.0335	0.0375
		74.0	0.0890	0.1004	0.0980	0.0915	0.0825	0.0645
		74.0	0.1080	0.1195	0.1180	0.1095	0.0975	0.0765
		74.0	0.1467	0.1595	0.1540	0.1435	0.1275	0.1005
		74.0	0.2198	0.2285	0.2200	0.2025	0.1805	0.1425

APPENDIX B (Continued)

Spacing Ident.	Slope	Temperature °F	Discharge (cfs)	Station Depths of Flow (Ft)				
				0 + 00	0 + 05	0 + 10	0 + 15	0 + 20
S-2	0.0104	74.0	0.0394	0.0370	0.0375	0.0405	0.0380	0.0410
		74.0	0.0775	0.0660	0.0690	0.0705	0.0690	0.0690
		74.0	0.1154	0.0970	0.0990	0.1005	0.0980	0.0950
		74.0	0.1792	0.1480	0.1500	0.1515	0.1470	0.1320
		75.0	0.2037	0.1700	0.1710	0.1705	0.1620	0.1460
D-2	0.0023	76.0	0.0205	0.0655	0.0675	0.0655	0.0605	0.0475
		76.0	0.0377	0.1095	0.1075	0.1015	0.0915	0.0685
		76.5	0.0541	0.1425	0.1385	0.1280	0.1130	0.0855
		76.5	0.0726	0.1755	0.1675	0.1545	0.1355	0.1085
		76.5	0.1005	0.2155	0.2065	0.1905	0.1690	0.1275
D-2	0.0045	75.0	0.0205	0.0380	0.0490	0.0470	0.0460	0.0380
		75.0	0.0670	0.1250	0.1310	0.1220	0.1120	0.0870
		75.0	0.0801	0.1560	0.1510	0.1410	0.1270	0.0990
		75.0	0.0934	0.1630	0.1640	0.1580	0.1430	0.1105
		75.0	0.1282	0.2170	0.2115	0.1910	0.1810	0.1390
D-2	0.0096	75.0	0.0279	0.0410	0.0445	0.0450	0.0405	0.0400
		75.0	0.0572	0.0840	0.0860	0.0850	0.0790	0.0705
		75.0	0.0897	0.1280	0.1290	0.1250	0.1170	0.1005
		76.0	0.1161	0.1650	0.1650	0.1580	0.1470	0.1230
		76.0	0.1438	0.2030	0.2010	0.1920	0.1750	0.1440
S-1	0.0021	65.0	0.0154	0.0750	0.0740	0.0710	0.0620	0.0470
		65.0	0.0286	0.1330	0.1200	0.1120	0.0940	0.0680
		65.0	0.0393	0.1580	0.1500	0.1370	0.1260	0.0870
		65.0	0.0467	0.1780	0.1680	0.1530	0.1300	0.0920
		65.0	0.0564	0.2000	0.1900	0.1720	0.1420	0.1280

APPENDIX B (Continued)

Spacing Ident.	Slope	Temperature °F	Discharge (cfs)	Station Depths of Flow (Ft)				
				0 + 00	0 + 05	0 + 10	0 + 15	0 + 20
S-1	0.0045	67.0	0.0155	0.0490	0.0520	0.0510	0.0360	0.0370
		67.0	0.0386	0.1240	0.1220	0.1150	0.0970	0.0730
		67.0	0.0468	0.1460	0.1420	0.1320	0.1120	0.0830
		67.5	0.0623	0.1810	0.1740	0.1590	0.1340	0.1000
		67.5	0.0714	0.1990	0.1910	0.1740	0.1510	0.1370
S-1	0.0104	63.5	0.0336	0.0710	0.0780	0.0790	0.0780	0.0645
		64.0	0.0484	0.1010	0.1080	0.1100	0.1040	0.0830
		64.0	0.0604	0.1230	0.1310	0.1310	0.1220	0.0990
		64.0	0.0783	0.1540	0.1620	0.1600	0.1470	0.1190
		64.5	0.1075	0.2060	0.2120	0.2050	0.1870	0.1480
D-1	0.0044	67.0	0.0134	0.0810	0.0720	0.0680	0.0650	0.0460
		67.0	0.0250	0.1290	0.1190	0.1110	0.1030	0.0730
		67.0	0.0304	0.1530	0.1410	0.1280	0.1190	0.0850
		67.0	0.0370	0.1800	0.1670	0.1530	0.1330	0.0975
		67.0	0.0476	0.2160	0.1990	0.1830	0.1665	0.1160
D-1	0.0097	68.0	0.0218	0.0800	0.0670	0.0830	0.0760	0.0630
		68.0	0.0339	0.1240	0.1150	0.1220	0.1110	0.0870
		68.0	0.0412	0.1470	0.1380	0.1440	0.1300	0.1000
		68.0	0.0482	0.1690	0.1530	0.1630	0.1420	0.1120
		68.0	0.0593	0.2030	0.1860	0.1930	0.1740	0.1330
S- $\frac{1}{2}$	0.0020	67.0	0.0065	0.0800	0.0790	0.0715	0.0590	0.0310
		67.0	0.0114	0.1230	0.1190	0.1070	0.0880	0.0470
		67.0	0.0167	0.1660	0.1570	0.1400	0.1150	0.0620
		67.0	0.0236	0.2190	0.2050	0.1820	0.1490	0.0770
		67.0	0.0269	0.2390	0.2230	0.1970	0.1600	0.0820

APPENDIX B (Continued)

Spacing Ident.	Slope	Temperature °F	Discharge (cfs)	Station Depth of Flow (Ft)				
				0 + 00	0 + 05	0 + 10	0 + 15	0 + 20
S-½	0.0047	67.5	0.0075	0.0640	0.0690	0.0840	0.0820	0.0765
		67.0	0.0202	0.1630	0.1580	0.1460	0.1240	0.0695
		67.0	0.0146	0.1210	0.1190	0.1120	0.0960	0.0545
		66.5	0.0299	0.2290	0.2190	0.1990	0.1660	0.0905
		66.5	0.0350	0.2610	0.2480	0.2250	0.1870	0.1035
S-½	0.0101	67.0	0.0170	0.0990	0.0995	0.0960	0.0890	0.0560
		67.0	0.0247	0.1450	0.1435	0.1370	0.1230	0.0730
		66.0	0.0385	0.2260	0.2195	0.2050	0.1790	0.1025
		65.0	0.0417	0.2400	0.2325	0.2170	0.1890	0.1090
		63.0	0.0321	0.1870	0.1825	0.1720	0.1520	0.0880

APPENDIX C

NOMENCLATURE

Symbol	Quantity	Dimensions
b	Channel width	ft
d	Diameter of roughness element	ft
y	Depth of flow	ft
E	Specific energy	ft
g	Acceleration due to gravity	ft/sec ²
H	Friction head	ft
H _v	Velocity head	ft
K	Stiffness modulus of element	lb-ft ²
l	Length of roughness element	ft
L	Length of test channel	ft
n	Manning's n, roughness coefficient	nonhomogeneous
R	Hydraulic radius	ft
R _e	Reynolds number	dimensionless
S _f	Energy slope	dimensionless
S _o	Channel bottom slope	dimensionless
V	Velocity of flow	ft/sec
x	Distance from some reference point	ft
Z	Bottom elevation above datum	ft
α	Coriolis velocity coefficient	dimensionless

λ	Shape factor defining type of roughness element	dimensionless
δ	Factor denoting roughness pattern	dimensionless
ρ	Fluid density	$\text{lb-sec}^2/\text{ft}^2$
μ	Fluid viscosity	$\text{lb-sec}/\text{ft}^2$

VITA

2
Timothy Soladoye Kowobari

Candidate for the Degree of
Master of Science

Thesis: HYDRAULIC EFFECT OF SIZE, SPACING AND PATTERN OF SPACING
OF ROUGHNESS ELEMENTS IN AN OPEN CHANNEL

Major Field: Agricultural Engineering

Biographical:

Personal Data: Born at Ijebu-Igbo, Western Nigeria, November 21,
1946, the son of Samson E. and Christianah T. Kowobari.

Education: Attended high school at Government College, Ibadan,
Western Nigeria, and graduated in December, 1964. Received
the Bachelor of Science degree in Agricultural Engineering
in August, 1968, from California State Polytechnic College,
San Luis Obispo. Completed the requirements for the Master
of Science degree in May, 1970.

Professional Experience: Temporary Agricultural Assistant,
Ministry of Agriculture and Natural Resources, Ibadan,
Western Nigeria, January to August, 1965; Graduate
Research Assistant for one year for the Agricultural
Engineering Department, Oklahoma State University,
Stillwater, Oklahoma, January, 1969, to January, 1970.

Professional Organization: Member of American Society of
Agricultural Engineers.